PONTIFICIA UNIVERSIDAD CATÓLICA DE CHILE
Doctorado en Neurociencias

Tesis Doctoral

THE C-ABL KINASE CONTRIBUTES TO THE COGNITIVE IMPAIRMENT OF TRANSGENIC ALZHEIMER'S DISEASE MICE.

Por

RILDA LEÓN MARTÍNEZ

Noviembre 2020

PONTIFICIA UNIVERSIDAD CATÓLICA DE CHILE
Doctorado en Neurociencias

Tesis Doctoral

THE C-ABL KINASE CONTRIBUTES TO THE COGNITIVE IMPAIRMENT OF TRANSGENIC ALZHEIMER'S DISEASE MICE.

Tesis presentada a la Pontificia Universidad Católica de Chile en cumplimiento parcial de los requisitos para optar al grado de Doctor en Neurociencias

Por

RILDA LEÓN MARTÍNEZ

Director de Tesis: Alejandra Álvarez

Comisión de Tesis: Rommy von Bernhardi
Waldo Cerpa
José Luis Valdés

Noviembre 2020

PONTIFICIA UNIVERSIDAD CATÓLICA DE CHILE
Doctorado en Neurociencias

El Comité de Tesis, constituido por los Profesores abajo firmantes, aprueba la Defensa Publica de la Tesis Doctoral titulada:

THE C-ABL KINASE CONTRIBUTES TO THE COGNITIVE IMPAIRMENT OF TRANSGENIC ALZHEIMER'S DISEASE MICE

Aprobación Defensa:

RILDA LEON MARTINEZ

Calificándose el trabajo realizado, el manuscrito sometido y la defensa oral, con nota

6,3 (seis coma tres)

Dr. Mauricio Cuello
Director de Investigación y Doctorado
Escuela de Medicina
Pontificia Universidad Católica de Chile

Dr. Felipe Heusser R.
Decano
Facultad de Medicina
Pontificia Universidad Católica de Chile

Dra. Claudia Sáez
Sub-Directora
Dirección de Investigación y Doctorado
Escuela de Medicina
Pontificia Universidad Católica de Chile

Dr. Francisco Aboitiz D.
Jefe Programa Doctorado en Neurociencias
Facultad de Medicina
Pontificia Universidad Católica de Chile

Prof. Alejandra Álvarez
Directora de Tesis
Facultad de Biología
Pontificia Universidad Católica de Chile

Prof. Rommy von Bernhardi
Profesor Evaluador Interno
Facultad de Medicina
Pontificia Universidad Católica de Chile

Dr. José Valdés
Profesor Evalualador Externo
Facultad de Medicina
Universidad de Chile

Prof. Waldo Cerpa
Profesor Evaluador Interno
Facultad de Ciencias Biológicas
Pontificia Universidad Católica de Chile

Santiago, 23 de noviembre de 2020

AGRADECIMIENTOS

He aquí el resultado final de 4 años de esfuerzo y de aprendizaje. Se cierra una etapa importante de mi formación profesional y de mi vida personal y es el momento ideal para agradecer a todas las personas involucradas.

Agradecer al Centro Interdisciplinario de Neurociencias. A los profesores de la comisión, por su contribución en el desarrollo de esta tesis. A la ANID por su financiamiento (Beca Doctorado Nacional 2016 - 21160057).

Agradecer a mi tutora, la Dra. Alejandra Álvarez. Gracias profe por aceptarme en su laboratorio y por aceptar mi idea de tesis, gracias por darme las fuerzas necesarias para terminar unos de los momentos más duro del doctorado. Gracias por toda la enseñanza académica y profesional.

También quiero agradecer a todos mis compañeros del Laboratorio de Señalización Celular. Todos han sido un aporte importante en mi formación. Del laboratorio hay 2 personas particularmente especial, la Dani y la Ame, que más que compañeras son amigas.

Y hablando de amigos, tengo una lista infinita a los cuáles agradecer. Sol y Marcos, mis primeros amigos en Chile, 2 personas bellas e incondicionales. ¿Qué hubiese sido de mi sin ellos? Alexandra, nos conocimos en el lugar incorrecto, pero en el momento perfecto. Nuestra amistad ha crecido y hemos sido soporte vital una de la otra. La Cata, primero compañera de laboratorio, luego amiga de las que hablan horas sin parar. Cristian, Coté, David, Mei-Li, Vicente, todos han sido importantes en este proceso de formación.

Finalmente quiero agradecer a mi familia. La familia que uno elige y la que no. Agradecer a mis papás, no han estado físicamente, pero están siempre presentes, preocupados y ocupados de mí. Son los mejores papás, no porque sean perfectos, nadie lo es, si no porque siempre han estado para mi dando más de lo que tienen. Y soy dichosa porque tengo otro padre, Alberto, que ha estado en mi vida por más de 20 años y siempre ha apostado por mí, sé que está orgulloso de este logro.

De la familia que uno escoge están Patry y Celia. Son esas amigas que te regala la vida, que un día deciden que serán amigas y de pronto, 13 años después, siguen ahí, siendo parte de tu vida, apoyándote en todo, en las duras y en las maduras. No importa si estamos en el mismo país o tenemos 14 horas de diferencia, siempre seremos nosotras 3. Y Miguel, que podría decirle a él que ya no le haya dicho. Mi compañero de mi vida, mi amor, mi amigo, gracias por todo el aguante y el apoyo.

TABLE OF CONTENT

AGRADECIMIENTOS 1
LIST OF FIGURES 4
LIST OF TABLES 5
LIST OF ABBREVIATIONS 6
RESUMEN 7
ABSTRACT 9
1 INTRODUCTION 11
1.1 Alzheimer's disease 11
1.2 Brain functional connectivity dysfunction in Alzheimer's disease 15
1.3 c-Abl role in the Central Nervous System 21
1.4 c-Abl and Alzheimer's disease 22
2 HYPOTHESIS 27
3 OBJECTIVES 28
4 MATERIALS AND METHODS 29
4.1 Animals 29
4.2 Experimental Design 31
4.3 Behavioral testing 33
4.4 Electrophysiological analysis 36
4.5 Immunofluorescence staining 43
4.6 Statistics 44
5 RESULTS 46
5.1 Objective 1. Evaluate the effect of the absence of c-Abl on learning and memory in APP/PS1-Abl-KO mice. 46
5.2 Objective 2. Evaluate the effect of the absence of c-Abl on functional connectivity between the Prefrontal Cortex and Hippocampus in APP/PS1-Abl-KO mice in resting-state 57
5.3 Objective 3. Assess the effect of the absence of c-Abl on β-amyloid plaques in APP/PS1/Abl-KO mice 68
6 DISCUSSION 70
6.1 Lack of c-Abl improves behavioral performance in hippocampal-dependent tasks. 70

6.2 Lack of c-Abl modifies the functional connectivity during resting-state between the prefrontal cortex and hippocampus. 74

6.3 Lack of c-Abl slows down the accumulations of Aβ plaques in the brain of APP/PS1/Abl-KO mice. 80

6.4 Mechanism Proposal 81

7 CONCLUSIONS 84

8 APPENDIX 86

8.1 TABLE Nº1. Amplification programs for genotypification 86

8.2 TABLE Nº2. Primers sequences 86

8.3 Results corresponding to FIGURE Nº8 87

8.4 Results corresponding to FIGURE Nº3 88

9 REFERENCES 89

LIST OF FIGURES

FIGURE Nº1. Scheme of the experimental design. (Pag. 37)

FIGURE Nº2. Representative images from the recording sites. (Pag. 44)

FIGURE Nº3. Object Location Memory test. (Pag. 52)

FIGURE Nº4. Novel Object Recognition test. (Pag. 54)

FIGURE Nº5. Barnes Maze test. (Pag. 56)

FIGURE Nº6. Open Field test. (Pag. 58)

FIGURE Nº7. Memory Flexibility test. (Pag. 61)

FIGURE Nº8. Neuronal activity in the Prefrontal Cortex. (Pag. 64)

FIGURE Nº9. Sharp-wave ripples parameters. (Pag. 67)

FIGURE Nº10. Cross-correlation analysis. (Pag. 70)

FIGURE Nº11. Coherence analysis. (Pag. 72)

FIGURE Nº12. Amyloid burden quantification. (Pag. 74)

FIGURE Nº13. Mechanism Proposal. (Pag. 89)

SUPPLEMENTARY Nº1. Waveform characteristics of putative pyramidal cells and putative interneurons recording from medial PCF. (Pag. 93)

SUPPLEMENTARY Nº2. Object Location Memory test in young mice. (Pag. 94)

LIST OF TABLES

TABLE Nº1. Amplification programs for genotypification. (Pag. 92)

TABLE Nº2. Primers sequences. (Pag. 92)

LIST OF ABBREVIATIONS

AD	Alzheimer's disease
Aβ	Amyloid-β peptide
APP	Amyloid Precursor Protein
AβO	Amyloid-β oligomers
AMPAR	α-amino-3-hydroxy-5-methyl-4-isoxazolepropionic acid receptor
BACE	β-site amyloid precursor protein cleaving enzyme
BM	Barnes Maze test
HPC	Hippocampus
LTP	Long Term Potentiation
MF	Memory Flexibility test
NOR	Novel Object Recognition test
NMDA	N-methyl-D-aspartate
NMDARs	N-methyl-D-aspartate receptors
OF	Open Field test
OLM	Object Location Memory test
PFC	Prefrontal Cortex
mPFC	Medial Prefrontal Cortex
SWRs	Sharp-wave ripples

RESUMEN

c-Abl es una tirosina quinasa que está involucrada en el desarrollo neuronal, neurogénesis, migración neuronal, extensión del axón y plasticidad sináptica. Crecientes evidencias posicionan a la c-Abl en un rol importante en la patología de la enfermedad de Alzheimer (EA). Nuestro laboratorio ha mostrado que c-Abl se activa en modelos *in vitro* e *in vivo* de la enfermedad, y su activación involucra pérdida sináptica e inhibición de la potenciación a largo plazo inducida por oligómeros Aβ. Además, el tratamiento con Imatinib, un inhibidor de c-Abl, reduce la pérdida neuronal, la hiper-fosforilación de tau y los depósitos Aβ. Mas importante aún el tratamiento con el inhibidor Imatinib disminuye el deterioro en el desempeño cognitivo de animales modelos de EA. No obstante, una de las limitaciones de estos estudios es que lo inhibidores empleados tienen una baja permeabilidad a la barrera hematoencefálica, además de inhibir a otras quinasas como blancos secundarios.

En este sentido, nos preguntamos si la c-Abl activada contribuye a la disminución de la conectividad funcional y al déficit cognitivo presente en un modelo animal de la Enfermedad de Alzheimer. Y si bien se ha descrito que en la EA hay alteraciones en la conectividad funcional, no se ha estudiado el rol de la c-Abl en la misma. Para responder a nuestra interrogante evaluamos el efecto de la ablación genética de c-Abl sobre el desempeño cognitivo y la conectividad funcional cortical, en un modelo de la EA. A partir del modelo de Alzheimer doble transgénico APP/PS1 y de la cepa Abl-KO, un ratón que permite la deleción de c-Abl específica en cerebro, generamos una nueva cepa transgénica: APP/PS1/Abl-KO. Así, evaluamos el desempeño cognitivo en cuatro grupos experimentales: WT, Abl-KO, APP/PS1 y APP/PS1/Abl-KO, a través de diferentes pruebas conductuales: Reconocimiento de objeto nuevo (NOR), Memoria de localización de objeto (OLM), Laberinto de Barnes (BM) y Flexibilidad de Memoria (MF). También evaluamos la actividad neuronal intrínseca y la conectividad funcional en el eje hipocampo-corteza prefrontal, para así establecer un correlato neuronal con las funciones cognitivas.

Los resultados mostraron que, en el OLM, una prueba dependiente de hipocampo, los animales nulos de c-Abl en el contexto de la enfermedad de Alzheimer (APP/PS1/Abl-KO) mejoraron su capacidad de reconocer el objeto desplazado. También, en el BM, otra prueba dependiente de hipocampo, los animales APP/PS1/Abl-KO encuentran más rápido la plataforma de escape. De manera similar, en el MF los animales APP/PS1/Abl-KO requieren menos intentos para alcanzar el criterio de aprendizaje. Estos resultados sugieren que c-Abl juega un rol deletéreo en la cognición en el contexto de la EA. Interesantemente, c-Abl parece jugar un efecto similar en la disfunción asociada al envejecimiento. Reflejado en la

mejora del desempeño cognitivo observada en los animales Abl-KO comparado con los animales WT en el OLM y el BM.

Los parámetros neurofisiológicos también mostraron diferencias marcadas entre los grupos experimentales. En el análisis de cros-correlación entre los *ripples* del hipocampo y las espigas de la corteza prefrontal encontramos que los animales APP/PS1 mostraron una hiperactividad patológica de la corteza prefrontal, la cual no está asociada con el aumento de la tasa de descarga en esta área. Esta hiperactividad disminuyó en los animales nulos de c-Abl en el contexto de la EA. Además, cuando evaluamos la actividad sincrónica entre la corteza y el hipocampo durante la oscilación theta, encontramos que los animales WT y APP/PS1/Abl-KO tenían significativamente mejor coherencia que los animales Abl-KO y APP/PS1. Mientras que los Abl-KO y los APP/PS1 no presentaban diferencia entre ellos. Ambos parámetros mencionados anteriormente son indicativos de la conectividad cerebral, sugiriendo así que la ausencia de c-Abl en el contexto de la EA fortalecería la conexión entre el hipocampo y la corteza prefrontal. Finalmente, el análisis histopatológico sugiere que la ausencia de c-Abl retrasa la acumulación de placas amiloides.

En resumen, el presente trabajo realiza dos aportes importantes al campo de estudio de la Enfermedad de Alzheimer. En primer lugar, confirma el rol de la c-Abl en la patología de la EA, que había sido previamente descrito con el uso de inhibidores. En segundo, lugar se describe la participación de la c-Abl en el déficit de la conectividad funcional presente en un modelo animal de EA. En conjunto, los resultados aquí presentados entregan un poderoso respaldo para considerar a la c-Abl un probable blanco terapéutico para el tratamiento de la enfermedad.

ABSTRACT

c-Abl is a non-receptor tyrosine kinase involved in neuronal development, neurogenesis, neuronal migration, axonal extension, and synaptic plasticity. Growing evidence suggests that c-Abl plays a role in the pathogenesis of Alzheimer's disease (AD). Our laboratory has shown that c-Abl is activated in both *in vitro* and *in vivo* AD models, and its activation is involved in synaptic loss and long-term potentiation inhibition induced by Aβ oligomers. Also, Imatinib treatment, a c-Abl inhibitor, reduces neuronal loss, tau phosphorylation, Aβ deposition, and improves the cognitive performance in transgenic AD mouse models. However, one of the limitations of those studies is that inhibitors have low permeability of the blood-brain barrier and target other kinases.

There is no evidence of how the c-Abl effect at the molecular level influences the behavioral performance. In this sense, we wonder if the c-Abl contributes to decreased functional connectivity and cognitive decline in a transgenic Alzheimer's disease model. To address the question, we assessed the effect of the genetic ablation of c-Abl on cognitive performance and functional cortical connectivity in a transgenic AD mouse model. Using the APP/PS1 and Abl-KO, we generated a new transgenic strain of AD, APP/PS1/Abl-KO with a brain-specific genetic deletion of c-Abl. We evaluated the cognitive performance of four experimental groups WT, Abl-KO, APP/PS1 y APP/PS1/Abl-KO, using different behavioral tests: Novel Object Recognition (NOR), Object-Location Memory (OLM), Barnes Maze test (BM), and Memory Flexibility (MF). We evaluated the intrinsic neuronal activity and functional connectivity in the hippocampal-prefrontal cortex axis to establish neural correlates of cognitive function in the transgenic lines.

We found in the OLM test, a hippocampus-dependent task, that mice null for c-Abl in AD (APP/PS1/Abl-KO) had improved the ability to recognize the displaced object. Also, in the BM test, another hippocampus-dependent test, the APP/PS1/Abl-KO mice learned faster than the others. Similarly, in the MF test, APP/PS1/Abl-KO mice required fewer trials to reach the learning criterion. These results suggest that c-Abl plays a detrimental role in cognition in the context of AD pathology. Interestingly, c-Abl seems to play a similar effect on the dysfunction associated with aging. Abl-KO mice had better performance than WT mice in the OLM and BM tests.

Neurophysiological parameters also showed distinct differences between groups. In the cross-correlation analysis between hippocampal SWRs and mPFC spikes, we found that APP/PS1 mice showed pathological hyperactivity of the prefrontal cortex, not associated with the firing rate. This hyperactivity was decreased in animals lacking c-Abl in the context of AD. Also, when we evaluated synchronous activity

between Prefrontal Cortex and Hippocampus during theta oscillations, we found that WT and APP/PS1/Abl-KO groups were significative different from Abl-KO and APP/PS1. In contrast, Abl-KO mice had no differences with APP/PS1 mice. Both parameters mentioned earlier are indicative of cortical connectivity; thus, the lack of c-Abl strengthener this connection in the context of Alzheimer's disease. Finally, the histopathological analysis suggests that the lack of c-Abl delay amyloid plaque accumulation.

In summary, the present work makes two significant contributions in the field of study of AD. In the first place, confirm the role of c-Abl on Alzheimer's disease's pathological mechanism. Second, described c-Abl participation in the decreased functional connectivity seems in an animal model of AD. Taken together, the results presented here provide full support to consider the c-Abl as a feasible therapeutic target in Alzheimer's disease.

1 INTRODUCTION

1.1 Alzheimer's disease

Alzheimer's disease (AD) is a neurodegenerative illness characterized by cognitive decline, primarily affecting memory (Scott et al., 2012). Alzheimer's disease is the leading form of dementia worldwide and may contribute to 60–70% of cases (*Dementia*, n.d.). Most AD cases are sporadic (sAD), and multiple risk factors, such as aging, environmental stress, and diet, are thought to play critical pathogenic roles (Dorszewska et al., 2016). The remaining AD cases, which account for 5-10% of total AD cases, are inherited from one generation to the next and are referred to as familial AD (fAD) (Lane et al., 2018). The brains of patients with AD have a loss of neuronal populations in regions related to memory and cognition. The earliest AD changes are neuronal dysfunction (reduced connectivity and loss of plasticity) followed by synapsis loss, neurotransmitter depletion, cytoskeletal alterations, abnormal protein phosphorylation, and finally, neuronal death (Atwood & Bowen, 2015). Histopathologically, Alzheimer's disease shown extracellular accumulations of the amyloid-β peptide (Aβ), called amyloid plaques or senile plaques. It also has intracellular accumulations of neurofibrillary tangles (NFTs) (Atwood & Bowen, 2015).

In the first stage of AD, there is a progressive deficit in learning and short-term memory. Then, in later stages of the disease, long-term memories are impaired (Alberici et al., 2014). Non-cognitive symptoms like disturbances in diurnal activity, aggressiveness, and symptoms of the affective and paranoid-schizophrenic disease are often associated with AD, which – unlike the cognitive symptoms – are not progressive (Bilkei-Gorzo, 2014). Memory impairment is not equally in AD patients; episodic memory, semantic memory, and implicit memory are affected less than new facts or memories (Reitz et al., 2011). The neurons of the hippocampus and the association areas involved in cognitive functions become increasingly dysfunctional, with loss of dendritic spines and synapses. Neurotransmitter pathways start to fail notably, not only the cholinergic system but also the glutamatergic and serotoninergic system (Xu et al., 2012). Progressive brain atrophy, particularly in the neocortex and hippocampus, is observed in magnetic resonance imaging scans from AD patients (Alberici et al., 2014).

1.1.1 Alzheimer's disease models

Experimental models play a crucial role in the understanding of different pathologies. Many models of Alzheimer's disease, *in vitro* and *in vivo*, are reported in the literature. Those are essential to understand AD pathogenesis further and perform pre-clinical testing of novel therapeutics. However, most experimental models almost exclusively consist of transgenic mice that express human AD-associated genes that result in the formation of amyloid plaques.

Mouse APP has 97% sequence homology with human APP. Notably, sequence differences between mice and humans include three amino acids within the Aβ sequence. These differences reduce Aβ aggregation and prevent the formation of amyloid plaques in wild-type mice. Therefore, human APP expression is necessary to form amyloid plaques in mice (Drummond & Wisniewski, 2017). Mice that overexpress genes for a human APP with fAD mutations, alone or in combination with mutant human presenilin 1 (PSEN1) gene are the most useful AD research models (Drummond & Wisniewski, 2017).

In this sense, the widespread AD transgenic mouse model is the APPswe/PSEN1ΔE9, a double transgenic mouse that expresses a chimeric mouse/human mutant amyloid precursor protein (Mo/HuAPP695swe) and a mutant human presenilin 1 (PSEN1ΔE9) both directed to Central Nervous System neurons (Jankowsky et al., 2004). Both mutations are associated with early-onset AD. The transgenic mice develop Aβ deposits in the brain by 4-months-old, with a progressive increase of Aβ levels and plaque numbers of up to 12 months. Those increases are mainly in the cortex and Hippocampus (Finnie et al., 2017; Garcia-Alloza et al., 2006). Between 8 and 10 months is observed neuronal loss adjacent to plaques relative to more distal areas (Jackson et al., 2016).

Synaptic damage has also been seen in APPswe/PSEN1ΔE9 mice. In 2,5 month-old mice, a decrease in the synaptic density and a reduction in the postsynaptic density thickness are observed (Meng et al., 2017a). A decrease in pre-and postsynaptic components has also been reported, such as synaptophysin and NR2B, respectively (Meng et al., 2017b). Deficits in synaptic plasticity have been

observed, particularly deficits in transient long-term potentiation in mice from 3 to 12-months-old (Volianskis et al., 2010), as well as a decreased in dendritic spines in the dentate gyrus, CA1 and CA2/3 regions of the Hippocampus (Ma et al., 2020).There is very little information about brain connectivity in the APPswe/PSEN1ΔE9 model of Alzheimer's disease. However, using an imaging technique, Bero and colleagues demonstrate that Aβ deposition is associated with significantly reduced bilateral functional connectivity in multiple brain regions of older APPswe/PSEN1ΔE9 transgenic mice (Bero et al., 2012).

In APPswe/PSEN1ΔE9 mouse have been described deficits across cognitive and non-cognitive domains, although severity and timing depend on the specific behavioral protocols used (Janus et al., 2015; Zhang et al., 2018). 6-months-old mice showed contextual memory impaired in fear-conditioning tests (Kilgore et al., 2010). Additionally, from 9-months-old APPswe/PSEN1ΔE9 mice showed impairment in spatial learning during the acquisition and the probe trial in the Morris Water Maze (Lalonde et al., 2005; Ma et al., 2011; Zhong et al., 2014). Besides, there have been reported deficits in other hippocampus-dependent tasks such a Barnes Maze (Cheng et al., 2019; Reiserer et al., 2007) and Object Location Memory (Sierksma et al., 2014).

In this thesis, we use the APPswe/PSEN1ΔE9 because it is a model that reproduces with reasonable accuracy the development of the disease in humans. As mentioned above, this model accumulates plaques progressively. It also shows a cognitive impairment in an age-dependent manner (Liu et al., 2017).

1.2 Brain functional connectivity dysfunction in Alzheimer's disease

Functional connectivity means that spatially separated brain regions have a simultaneous activation. This functional connectivity is observed when performing any cognitive task but also during rest-state. The abnormalities in functional connectivity eventually lead to abnormalities in each brain region activity, resulting in cognitive dysfunction (Lee et al., 2020). Some reports have evaluated the functional connectivity in AD patients (Anderkova et al., 2017; Wood, 2014).

Studies have shown that dementia severity correlates with alterations on the default mode network and other resting-states networks. Accordingly, reduced functional connectivity correlates with a worse Clinical Dementia Rating (Brier et al., 2012). Also, alterations in functional connectivity have been seen in both sporadic and familial AD (Wood, 2014), as well as resting-state striatum-cortical connectivity has been negatively correlated with memory performance in AD patients (Anderkova et al., 2017). Additionally, an inability to switch out of states of low inter-network connectivity into more highly and especially connected network configurations might be related to the presence of dementia (Schumacher et al., 2019). Further, AD patients have increased static functional network connectivity (sFNC) between the visual and cerebellar (CB) domains but decreased sFNC between the default-mode and CB domains (Fu et al., 2019). In the early stage of AD, patients show hyperexcitability of the network. A recent study shows that the hypersynchrony predicts conversion, leading to a network breakdown in progressive Mild Cognitive Impairment (Pusil et al., 2019). Earlier, Vossel and colleagues described a subclinical epileptiform activity in almost half of their study's AD patients. Those

patients showed faster declines in global cognition, determined by the Mini-Mental State Examination (Vossel et al., 2016). Thus, patients with network hyperexcitability are at risk for accelerated cognitive decline. Moreover, a study in healthy young humans that carried out the APOE-ε4, the most significant genetic risk for AD, found increased connectivity across frequencies, concluding that the initial hyper-connectivity leads to a late disconnection, suggesting that this is present decades before the onset of AD symptomology (Koelewijn et al., 2019).

The Hippocampus-Prefrontal Cortex interaction is particularly relevant in Alzheimer's disease. The Hippocampus and PFC interact in a bidirectional manner to regulate several cognitive functions. These structures are involved in the memory system, facilitating fast encoding of new information, consolidation, retrieval, and organization of the memory network (Zielinski et al., 2019). In early-stages AD patients has been describe that in resting-state, the functional connectivity between Hippocampus and Prefrontal cortex is disrupted (Wang et al., 2006). Also, images analysis during a face-memory task indicated that memory deficits early in AD were due to a reduction in the integrated network activity, with the PFC and Hippocampus as principal components (Grady et al., 2001)

In consonance with the latest findings related to functional connectivity in AD patients, in an AD mouse model has been demonstrated that Aβ deposition is associated with significantly reduced bilateral functional connectivity in multiple brain regions of older mice (Bero et al., 2012). A whole-brain seed analysis revealed a general decrease in functional connectivity in the brains of AD transgenic mice compared to wild-type mice. The interhemispheric functional connectivity is relatively

preserved in the transgenic mice's motor cortex but decreased in the somatosensory cortex and the hippocampus compared to the wild-type mice (Shah et al., 2013). Pre-clinical studies on neuronal impairments associated with progressive amyloidosis have demonstrated some Aβ-dependent neuronal dysfunction. In the early stages of disease progression, concomitant to amyloid deposition and tau hyperphosphorylation, transgenic animals showed a strongly attenuated power at low-gamma band in the HPC and mPFC. Besides, the phase-amplitude coupling of the neuronal networks in both areas was impaired (Bazzigaluppi et al., 2018).

The network hyperexcitability has also been described in AD models. Busche and colleagues found a marked increase in the fractions of hyperactive neurons in Hippocampus CA1 and cortex. Also, in the hippocampus of young mice, they observed a selective increase in hyperactive neurons already before the formation of plaques (Busche et al., 2012). Ghatak and colleagues also found this hyperexcitable pattern in human induced pluripotent stem cell (hiPSC)-derived cerebrocortical neuronal cultures and cerebral organoids bearing AD-related mutations. They found increased excitatory bursting activity, which could be explained partly by a decrease in neurite length. AD hiPSC-derived neurons also displayed increased sodium current density and increased excitatory and decreased inhibitory synaptic activity (Ghatak et al., 2019). Another study uses a mouse model of Aβ-amyloidosis to show that the suppression of glutamate reuptake initiates hyperactivation. They found that hyperactivity occurred in neurons with preexisting baseline activity, whereas inactive neurons were generally resistant to Aβ-mediated hyperactivation (Zott et al., 2019).

1.2.1 Molecular mechanism of the synaptic dysfunction

According to the Amyloid Hypothesis, the amyloid accumulation has been postulated as the leading cause of the neuronal dysfunction present in Alzheimer's disease. As earlier as 1993, Saito and colleagues described that the calcium-activated neutral proteinase (Calpain) activation ratio was elevated 3-fold in the prefrontal cortex of Alzheimer's disease patients. They concluded that Calpain activation might contribute to neurofibrillary pathology and abnormal APP processing before causing synapse loss or cell death (Saito et al., 1993). Many researchers have been postulated that the neuronal dysregulation of calcium homeostasis is an aspect that appears to be intimately involved in the AD neuronal dysfunction. Bai and colleagues show that abnormal dendritic calcium transients and synaptic depotentiation occur before amyloid plaque formation in a mouse model of AD (Bai et al., 2017). Also, in cultured neurons, AβO-stimulated calcium entry via NMDA receptors and drives neuronal death in AD (Kodis et al., 2018).

Aβ oligomers (AβO) target the postsynaptic compartment of excitatory synapses with high affinity, altering the structure, composition, and function of synapses (Koffie et al., 2009). Also, the pathological response induced by Aβ is abolished in NMDAR knockdown neurons. Significantly, knockdown of NMDARs abolished the binding of Aβ oligomers to dendrites, suggesting that NMDARs might be the targets of oligomer binding. However, additional results indicated that, although required for dendritic targeting of Aβ oligomers, NMDARs are likely not the mainly only molecules to which oligomers directly bind (Decker et al., 2010). Furthermore, Aβ facilitates the removal of AMPA receptors from the synaptic membrane, leading to synaptic depression

(Guntupalli et al., 2017). Alterations in long-term potentiation (LTP) is also described in different AD models (Oddo et al., 2003; Rezaeiasl et al., 2019; Vargas et al., 2014). Synaptic dysfunction, including LTP deficits, manifests in an age-related manner, but before plaque and tangle pathology. Deficits in long-term synaptic plasticity correlate with the accumulation of intraneuronal Aβ (Oddo et al., 2003).

On the other hand, other actors involved in the neuronal dysfunction present in AD have been described beyond amyloid or tau. A study showed aberrant mitochondrial function in patient-derived cells. They found that neuronal cultures from some patients produced more reactive oxygen species and presented higher levels of DNA damage. Besides, patient-derived cells showed increased levels of oxidative phosphorylation chain complexes, whereas mitochondrial fission and fusion proteins were not affected. Surprisingly, these effects neither correlated with Aβ nor phosphorylated and total tau levels (Birnbaum et al., 2018).

Deficits in functional connectivity are thought to occur due to synaptic alterations (Mucke & Selkoe, 2012). Xia et al. describe that excitatory synapses dependent on GluA4 are regulated by presynaptic expression of the early gene NPTX2. In a mouse model of AD amyloidosis, $Nptx2^{-/-}$ results in reduced GluA4 expression and disrupted rhythmicity. (Xiao et al., 2017). Another described mechanism of Aβ-induced synaptic injury is related to APP cleavage at position D664 by caspases that release the putatively cytotoxic C31 peptide. Loss of dendritic spines is attenuated in mice treated with caspase inhibitors. Significantly, the time-dependent dendritic spine loss is correlated with localized activation of caspase-3 but is absent in APP D664A cultures (Park et al., 2020).

A more classic mechanism is related to the cellular prion protein (PrP^C). The PrP^C acts as a receptor for Aβ42 oligomers mediating Aβ42-oligomer inhibition of synaptic plasticity in hippocampal slices (Laurén et al., 2009). Also, it has been shown that soluble Aβ binds to PrP^C at neuronal dendritic spines *in vivo* and *in vitro*, where it forms a complex with Fyn (Larson et al., 2012). Aβ engagement of PrP^C-Fyn signaling produces phosphorylation of the NR2B subunit of NMDA receptors, which was connected to an initial increase and then a loss of surface NMDARs (Um et al., 2012). Deletion of PrP^C expression in an animal model of AD rescues axonal degeneration, loss of synaptic markers, and no detectable impairment of spatial learning and memory, whereas the AD transgenic mice with intact PrP^C expression exhibit deficits in spatial learning and memory (Gimbel et al., 2010).

The EphA4 receptor is another candidate to explain the synaptic dysfunction in AD. It has been shown that the postsynaptic EphA4 is responsible for mediating synaptic plasticity impairment in AD (Fu et al., 2014; Vargas et al., 2014). There is an association between reducing hippocampal EphA4 and the impairment in object recognition and spatial memory test in animals AD models (Simón et al., 2009). Also, the EphA4 co-localizes with neuritic plaques in the hippocampus of AD patients and correlates with AD pathology hallmarks (Rosenberger et al., 2014).

Recently, a new hypothesis proposes that GABAergic dysfunction in excitatory and inhibitory balance drives Alzheimer's disease (Bi et al., 2020). The relationship between Aβ and neural activity may be the mechanism underlying Aβ-induced perisomatic GABAergic terminal loss. Microglia also actively modulates neuronal functions via morphological remodeling (Bi et al., 2020).

1.3 c-Abl role in the Central Nervous System

The non-receptor tyrosine kinase c-Abl is the cellular homolog of the transforming element of the Abelson murine leukemia virus, and its genetic rearrangement is the cause of chronic myelogenous leukemia. In addition to its classic function in leukemia pathogenesis, the Abl kinases are highly regulated by diverse stimuli that involve growth factors, chemokines, DNA damage, oxidative stress, and adhesion receptors (Wang, 2014). Abl kinases activation regulates signaling pathways implicated in the cytoskeletal reorganization that are important for cellular protrusions, cell migration, morphogenesis, adhesion, endocytosis, and phagocytosis (Wang, 2014). Abl kinases can also regulate cell survival and proliferation pathways, depending on the cellular context (Khatri et al., 2016).

c-Abl is present in different subcellular compartments, and the prominent locations are the cytoplasm and nucleus, but it is also in the mitochondria and the endoplasmic reticulum (Ito et al., 2001; Wetzler et al., 1993). c-Abl shifted cellular locations in response to extra- and intracellular signals and can translate and integrate different physiological and pathological stimuli in cell responses (Estrada & Alvarez, 2011). In the nucleus, c-Abl has a crucial role in selecting between cell cycle arrest and apoptosis in response to DNA damage. Nuclear c-Abl interacts with transcription factors such as p53 and p73. Particularly, c-Abl regulates the p73 phosphorylation, stability, and ability to transactivate apoptosis promoting genes (Alvarez et al., 2004). Otherwise, cytoplasmic Abl tyrosine kinases (c-Abl and Arg: Abl-related gene) are important transducers of extracellular signals. In the cytoplasm, the Abl kinase family members translate information from growth factors and adhesion receptors at the

cell surface into the cytoskeletal structure, cell motility, and endocytosis (Wang, 2014). Despite its subcellular locations, c-Abl kinase plays a role in neuronal development, neurogenesis, neuronal migration, axonal extension, and synaptic plasticity (Estrada & Alvarez, 2011; Koleske et al., 1998; Moresco et al., 2003; Wills et al., 1999; Woodring et al., 2002).

c-Abl has been localized in the pre- and postsynaptic compartments of the synapses. A study shows that paired-pulse facilitation (PPF) was significantly reduced at the Schaffer collateral-CA1 excitatory synapses in hippocampal slices from Abl knockout mice compared with wild-type mice. Furthermore, the treatment of wild-type slices with the specific c-Abl inhibitor STI571 also reduced PPF. However, no differences in basal synaptic transmission, LTP, and long-term depression were found (Moresco et al., 2003). Nevertheless, our lab has shown that c-Abl deficiency increased transcription of synaptic plasticity-related genes such as actin cytoskeleton and AMPA receptor dynamic regulators (González et al., submitted). Also, in cultured neurons, a c-Abl deficiency increases dendritic spine density and synaptic clustering. Moreover, as a reflection of the synaptic changes, young c-Abl knock out mice show faster learning that wild-type mice in different cognitive tests such as Barnes Maze, Novel Object Recognition, and Water Maze (González et al., submitted).

1.4 c-Abl and Alzheimer's disease

While the activity of c-Abl is crucial for proper neuronal development, c-Abl remains relatively quiescent in healthy adult neurons, and there are few known functions of

c-Abl in fully differentiated neurons. In recent years has been described that c-Abl activation in the adult brain occurs in the context of neurodegenerative diseases.

The role of c-Abl has mostly been studied in AD, the most common neurodegenerative disorder (Estrada & Alvarez, 2011; Schlatterer et al., 2011; Vargas et al., 2018). Our laboratory is one of the most active groups in the study of c-Abl on AD. In 2004, Álvarez et al. showed that the Aβ induced the c-Abl activation in a culture of hippocampal neurons carrying the cell signals required to induce neuronal death by Aβ. The inhibition of c-Abl activity by Imatinib prevented neuronal death by apoptosis induced by Aβ (Alvarez et al., 2004). Moreover, the presence and activation of c-Abl in AD patient's brains have been described. The activated c-Abl was most abundant in the hippocampus and co-localized with AD pathology, including amyloid plaques in AD patient's brains (Jing et al., 2009). Cancino et al. 2008, showed the therapeutic potential of the selective c-Abl inhibitor Imatinib *in vivo* AD animal models. The intrahippocampal injection of Aβ fibrils in rats induced an increase in c-Abl immunoreactive cells in the hippocampal area near the lesion. Imatinib's chronic intraperitoneal administration reduced the behavioral deficits, apoptosis, and tau phosphorylation in both Aβ fibrils injected rats and APPswe/PSEN1ΔE9 mice. Besides, the Imatinib treatment also decreased the number and size of Aβ deposits and tau phosphorylation in the APPswe/PSEN1ΔE9 mice (Cancino et al., 2008). Also, in neurons treated with Aβ, the Imatinib treatment, the inhibition of c-Abl expression by shRNA, and the expression of a c-Abl kinase death mutant prevented tau phosphorylation (Cancino et al., 2011).

Furthermore, c-Abl inhibition with Imatinib or c-Abl knockdown decreased the HDAC2 levels, increasing the expression of several synaptic genes in AD models (Gonzalez-Zuñiga et al., 2014). In consonance with these, the intra-hippocampal injection of an HDAC inhibitor before fear conditioning can rescue age-related contextual fear memory impairments (Peleg et al., 2010). More interesting, the early stages of AD have impaired synaptic plasticity and synapse loss, and Vargas and colleagues showed that Aβ activates the c-Abl in dendritic spines of cultured hippocampal neurons and that c-Abl kinase activity is required for Aβ-induced synaptic loss. The ephrin A4 receptor (EphA4) tyrosine kinase, which has been implicated in synaptic changes, is upstream of c-Abl activation by Aβ. EphA4 tyrosine phosphorylation (activation) increase in cultured neurons and synaptoneurosomes exposed to Aβ, and in APPswe/PSEN1ΔE9 mice brain. The inhibition of EphA4 using the antagonist peptide KYL or the c-Abl inhibition by Imatinib prevents the dendritic spine reduction, blocking LTP induction and neuronal apoptosis caused by Aβ. Then EphA4/c-Abl activation is a key-signaling event that mediates the synaptic damage induced by Aβ (Vargas et al., 2014).

Recently, it was described the role of c-Abl on dendritic spine morphological changes induced by Aβ-oligomers (AβOs). In the presence of AβOs, c-Abl participates in synaptic contact removal, increasing susceptibility to AβOs damage. Its deficiency increases the immature spine population reducing AβOs-induced synapse elimination (Gutierrez et al., 2019).

c-Abl activation has been reported in both Parkinson's disease (PD) patients' brains and in mouse models of this disease. c-Abl activation is related to parkin substrates

accumulation and neuronal cell death. Administration of Nilotinib, a specific inhibitor of the c-Abl kinase, reduces the parkin substrates' levels, resulting in the prevention of dopamine neuron loss and behavioral deficits (Karuppagounder et al., 2014). Also, c-Abl regulates the degradation of parkin and α-synuclein (Mahul-Mellier et al., 2014). Administration of Nilotinib improves motor behavior, prevents the loss of dopamine neurons, regulates α-synuclein phosphorylation and clearance, inhibits the tyrosine phosphorylation of parkin, and decreases parkin substrate (Zhou et al., 2017). Also, c-Abl has been related to Amyotrophic Lateral Sclerosis (ALS). ALS transgenic mice showed upregulation of c-Abl in motor neurons, and the treatment with the c-Abl inhibitor Dasatinib decreased the activated caspase-3 levels in the lumbar spine, improved the innervation status of neuromuscular junctions, and increased the survival of these mice. Besides, c-Abl expression in postmortem spinal cord tissues from sporadic ALS patients was increased by 3-fold compared with non-ALS patients (Katsumata et al., 2012), and activated c-Abl increased in the brain and spinal cord of symptomatic mice model of ALS (Rojas et al., 2015).

Niemann-Pick type C (NPC) disease is a disorder characterized by the accumulation of free cholesterol. Those patients have markedly progressive neuronal loss, mainly of cerebellar Purkinje neurons. Results from our laboratory have shown that in an NPC1 mouse model, the proapoptotic c-Abl/p73 system and the p73 target genes are expressed in the cerebellums of NPC mice. Furthermore, NPC mice treated with Imatinib preserved Purkinje neurons, reduced general cell apoptosis in the cerebellum, improved neurological symptoms, and increased NPC mice survival (Alvarez et al., 2008). Also recently has been described the activation of c-Abl in

Epilepsy. Both the temporal cortex of patients with temporal lobe epilepsy (TLE) and in the hippocampus and cortex of a TLE rat model showed upregulation of both total and phosphorylated c-Abl (Chen et al., 2014).

Summarizing, in the present background, it has been describing that Alzheimer's disease leads to a memory deficit and impaired functional connectivity. The impaired functional connectivity is particularly relevant in the Prefrontal Cortex-Hippocampus axis because these structures are involved in the memory system, facilitating fast encoding, consolidation, and retrieval.

On the other hand, c-Abl has emerged as a key protein in AD pathology. However, the studies of c-Abl in the context of Alzheimer's disease have been carried out using c-Abl inhibitors. Most of these inhibitors are not selective to c-Abl, targeting other kinases. Therefore, the genetic deletion of c-Abl would be an ideal approach to clarify the role of c-Abl in AD's pathogenesis. There is evidence of how the c-Abl acts to worsen the disease at a molecular level. Results indicate that the treatment with a c-Abl inhibitor improves the cognitive performance of AD animal models. However, there is no evidence of how the c-Abl effect at the molecular level influences behavioral performance. Could be the functional connectivity the missing gap? Does the genetic deletion of c-Abl improve cognitive deficit and impaired functional connectivity present in an animal model of Alzheimer’s disease? The present work will intent to answer those questions.

2 HYPOTHESIS

Most studies related to c-Abl activation on AD's pathogenesis are using c-Abl inhibitors (Imatinib, Nilotinib, Dasatinib). As described above, our laboratory has made some contributions in the field, showing that the inhibition of c-Abl has a beneficial effect on AD pathology. However, most of these inhibitors cannot penetrate the blood-brain-barrier. Although some of them can penetrate it, they are not selective to c-Abl, targeting other kinases (Palakurti & Vadrevu, 2017). Therefore, genetic deletion of c-Abl would be an ideal approach to clarify if c-Abl is indeed an essential protein in AD's pathogenesis. There is evidence of how the c-Abl acts to worsening the disease at a molecular level (Alvarez et al., 2004; Cancino et al., 2008, 2011; Gonzalez-Zuñiga et al., 2014; Gutierrez et al., 2019). Other results indicate that Imatinib's treatment improves the cognitive performance of AD animal models (Cancino et al., 2008). However, there is no evidence of how the c-Abl effect at the molecular level influences behavioral performance. In this sense, we establish the hypothesis that **the c-Abl contributes to decreased functional connectivity and cognitive decline in a transgenic model of Alzheimer's disease**.

3 OBJECTIVES

General Objective

To evaluate the cognitive performance and functional connectivity in the Hippocampus-Prefrontal Cortex axis in transgenic models of Alzheimer's disease null of c-Abl.

Specific Objectives

1. Evaluate the effect of the absence of c-Abl on learning and memory in APP/PS1-Abl-KO mice.
2. Evaluate the effect of the absence of c-Abl on functional connectivity between the Prefrontal Cortex and Hippocampus in APP/PS1-Abl-KO mice in resting-state.
3. Assess the effect of the absence of c-Abl on β-amyloid plaques in APP/PS1/Abl-KO mice.

4 MATERIALS AND METHODS

4.1 Animals

Animals were maintained in the Animal Care Facility CIBEM of the Pontificia Universidad Católica de Chile (PUC), which follows the Guide for the Care and Use of Laboratory Animals published by NIH, USA. Animals were housed in a temperature and humidity-controlled room (22 ± 2°C) with food and water *ad libitum*. Experiments were carried out with 10-month-old mice approximately, except the Memory Flexibility test, that was carried out with 13-month-old mice. Protocols were approved by the Bioethics and Care of Laboratory Animals Committee of the Pontificia Universidad Católica de Chile, and CIBEM (Protocol ID 170616008).

c-Abl1-floxed ($Abl^{loxP/loxP}$) mice were kindly donated by Dr. AJ Koleske (Yale School of Medicine, US) and bred in our animal facility. Abl1-KO mice ($Abl^{loxP/loxP}$/Nestin-CRE) mice were bred from $Abl^{loxP/loxP}$ (these floxed mutant mice possess loxP sites flanking exon 5 of the Abl1 gene) mice and Nestin-CRE+ mice, which were obtained from Jackson Labs. This strain was originated and maintained on a mixed B6.129S4, C57BL/6 background and did not display any gross physical or behavioral abnormalities. This bread results in a brain-specific c-Abl null mouse. The genetic background is C57BL/6;C3H.

APPswe/PSEN1ΔE9 mice were purchased from Jackson Laboratory (Bar Harbor, ME, USA), number 34829-JAX. The trade name of the mouse is B6;C3-Tg(APPswe,PSEN1dE9)85Dbo/Mmjax. The genetic background is C57BL/6;C3H.

To obtain the four genotypes used in the present thesis, we initially bread APPswe/PSEN1ΔE9 mice with $Abl^{loxP/loxP}$ mice, resulting in APPswe/PSEN1ΔE9/$Abl^{loxP/loxP}$ mice. Then the APPswe/PSEN1ΔE9/$Abl^{loxP/loxP}$ mice were bred with $Abl^{loxP/loxP}$/Nestin-CRE mice, resulting in the four genotypes of interests: APPswe/PSEN1ΔE9/$Abl^{loxP/loxP}$ mice (APP/PS1, from now and on), APPswe/PSEN1ΔE9/$Abl^{loxP/loxP}$/Nestin-CRE mice (APP/PS1/Abl-KO, from now and on), $Abl^{loxP/loxP}$ mice (WT, from now and on), and $Abl^{loxP/loxP}$/Nestin-CRE mice (Abl-KO, from now and on).

The genotypes of all the animals were confirmed by polymerase chain reaction (PCR). Briefly, the mouse ear was punched, and the resulting piece was incubated overnight at 55ºC in lysis buffer [Tris-HCl 50 mM (pH 8), EDTA 100 mM, NaCl 100 mM, SDS 1%] supplemented with proteinase K 1%. After that, the samples were centrifuged, and 500 µl of isopropanol was added to the supernatant and mixed by inversion. After that, the mix was centrifuged again, and to the resulting sediment, 500 µl of ethanol was added. Subsequently, the ethanol was removed, and the sediment with DNA dried at room temperature. Finally, the DNA was resuspended in nuclease-free ultrapure distilled water. The PCR amplification was followed by the program detailed in the TABLE Nº1, Appendix section. The primer used and its sequence are listed in the TABLE Nº2 Appendix section.

4.2 Experimental Design

FIGURE Nº1 shows a scheme of the experimental design. Here we use a total of 40 animals, 16 females and 24 males. The animals were divided into four experimental groups: $Abl^{flox/flox}$ that we called WT (10 mice), $Abl^{floxflox}$/Nestin-CRE that is null for c-Abl in the neurons here called Abl-KO (11 mice), APP/PS1 (10 mice), APP/PS1/Abl-KO (9 mice). All the experiments were performed in the same set of animals except for the Memory Flexibility test. The Memory Flexibility test was not previously in the original project; however, we decided to add it to increase our data's robustness in the hippocampus-dependent task. To perform the Memory Flexibility test, we use a total of 28 animals, WT (8 mice), Abl-KO (6 mice), APP/PS1 (6 mice), and APP/PS1/Abl-KO (8).

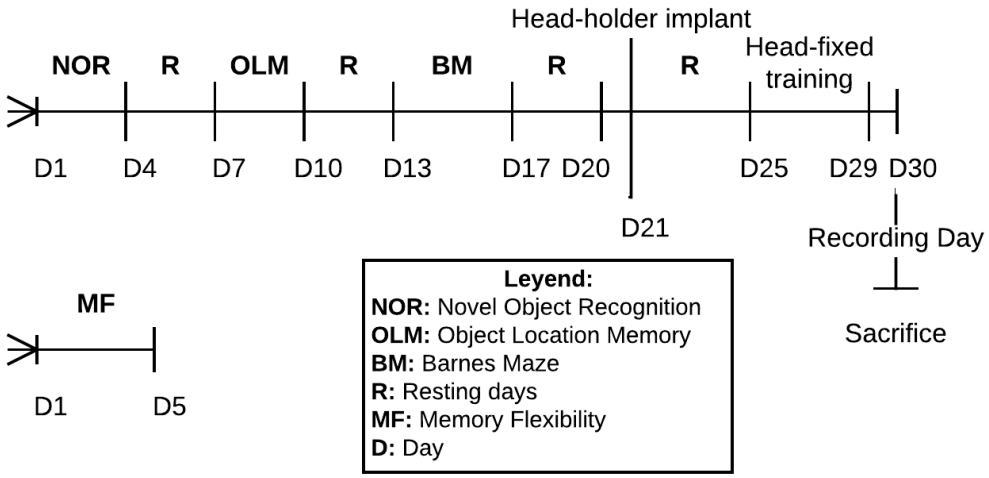

FIGURE Nº1. Scheme of the experimental design. Timeline of the experimental procedures. Four experimental groups were used in this work: WT, Abl-KO, APP/PS1, APP/PS1/Abl-KO. The details of each group are mentioned in the Material section. The Memory Flexibility test was not initially in the project; for this reason, it is in a different timeline. All the experiments were carried out in the same set of animals, except for the Memory Flexibility. Once the animal was sacrificed, the brain was reserved for immunofluorescence analysis. The mice started the experimental procedure with 10-month old approximately and finished the protocol at 11-month old approximately. The set of animals used to perform the Memory Flexibility tests were 12-month old approximately. NOR: Novel Object Recognition. OLM: Object Location Memory. BM: Barnes Maze. MF: Memory Flexibility. R: resting days. D: days.

4.3 Behavioral testing

Before behavioral testing, all animals were familiarized with the testing room. The behavioral tests were performed from less anxiogenic to most anxiogenic. Also, the tests were performed three days from each other to rest the animals.

4.3.1 Novel Object Recognition and Object Location Memory tests

The Novel Object Recognition (NOR) task evaluates the recognition memory, the rodent ability to recognize a novel object in the environment (Antunes & Biala, 2012). The task procedure consists of three sessions: habituation, sample, and test. The habituation session was repeated on two consecutive days. In the first habituation day, we recorded the animal's performance in the open field to evaluate the general activity levels, such as exploration habits and locomotor activity (Seibenhener & Wooten, 2015). In the habituation session, the mouse was placed in the empty open field, facing the wall that is nearest to the experimenter, and allow it to explore the open field for 10 minutes. Then the mouse was returned to its home cage. During the sample session, the identical to-be-familiarized objects were placed in the apparatus. The animal was positioned at the midpoint of the wall opposite the sample objects. After the sample-object exposure time (10 minutes), the animal was removed and returned to its home cage. The test session was performed 24 hours after the sample day. One familiar object and the novel object were placed in the apparatus. The testing session lasted for 5 minutes. The exploration time of both objects was measured and calculated the recognition index, RI (the time spent exploring the novel object relative to the total time spent exploring both objects). RI

above 0.5 means that the animal can differentiate the novel object from de familiar one. On the other hand, RI below 0.5 means that the animal cannot distinguish between objects.

The Object Location Memory (OLM) task is also a test that evaluates memory, particularly spatial memory (Murai et al., 2007). The task procedure of the OLM is like the NOR procedure. The difference consists that in the test session, one of the objects is displaced to a new position. In the OLM, the RI is interpreted as the capacity of the animal of recognized the displaced object. Another difference with the NOR is that the OLM task has intra-maze visual cues.

The maze used to perform Open Field, Novel Object Recognition, and Object Location Memory tests was a gray acrylic rectangular box (46cm x 27cm dimensions). The objects used in the Novel Object Recognition test and Object Location Memory test were previously equilibrated (to avoid innate preference) and were distinct in each test.

4.3.2 Barnes Maze

In this test, the animal should learn and remember the location of an escape hole in an anxiogenic, elevated, and illuminated circular open field (Barnes, 1979). We used the same protocol published in Negrón-Oyarzo et al., 2015. The maze is a white circular platform of 70-cm diameter elevated at 70 cm from the floor with 20 equally spaced holes along the perimeter (7-cm diameter each) located at 2 cm from the edge of the platform. The platform has 20 equally spaced holes along the perimeter. Visual cues were located on the walls of the room. Under one of the holes was

located a black plexiglass escape box (17 × 13 × 7 cm). The maze was illuminated with two incandescent lights to yield a light level of ~600 lux impinging on the circular platform. The location of the escape box was consistent for a given mouse but randomized across mice. Each mouse was given four trials per day with an intertrial interval (ITI) of 15 minutes during four consecutive days. The mouse was placed in the start box for every training trial for 10 seconds, with the room lights turned off. After time had elapsed, the chamber was lifted, the lights turned on, and the mouse was free to explore the maze. The session ended when the mouse found the hole and entered the escape box or after 3 minutes elapsed. When the mouse entered the escape box, the lights were turned off, and the mouse remained in the dark for 1 minute before the next trial began. If the mouse did not find the escape box within 3 minutes, the experimenter guided the mouse to the escape. We measured the latency to enter the escape box (Negrón-Oyarzo et al., 2015).

4.3.3 Memory Flexibility test

The Memory Flexibility test is a variation of the Morris Water Maze and has seen to be more sensitive to hippocampal dysfunction (Chen et al., 2000). The maze used was a white circular pool of 1.6 m of diameter and 75 cm deep. The pool's water was maintained at 19–21ºC and was colored with white dye to hide the platform. The platform was made of transparent acrylic (9 cm diameter) and was in the center of the corresponding quadrant. This test was performed as described by Toledo and Inestrosa, 2010. Each animal was trained in a circular water maze for four days. Each day of testing, the platform was changed to the next subsequent quadrant. The animal was considered to finish the training when reaching the criterion (three

consecutive trials with an escape latency less than 20 seconds) in each training day. The maximal trials per day were 15. Once the animal finished the test, it was removed from the maze, dried, and returned to its cage (Toledo & Inestrosa, 2010).

4.3.4 Data collection

All the behavioral tests, except for the Memory Flexibility test, were carried out in the Behavioral Room at the Animal Care facility of the Centro de Investigaciones Médicas at PUC. Each mouse's activity was recorded with a video camera (ImageLab, model CB3200) fixed above the behavioral apparatus connected to a computer. Videos were acquired by Lab View software and analyzed offline using the idTracker video-tracking software (Pérez-Escudero et al., 2014) and Matlab homemade scripts for the analyses. The Memory Flexibility test was performed in the Behavioral Room at the Departamento de Biología Celular y Molecular, PUC. The videos were acquired and analyzed using the ANY-maze video tracking system.

4.4 Electrophysiological analysis

After behavioral testing, mice were three days free until the beginning of the electrophysiological recordings.

4.4.1 Surgery for chronic implantation

Mice were anesthetized with isoflurane (5% induction and 1.5 – 2% maintenance) and placed on a stereotaxic frame (David Kopf Instruments). The temperature was kept at 37° throughout the procedure (1-2 hours) using a heating pad. The skin was incised to expose the skull and implanting a customized lightweight metal head-

holder. The holder was glued to the bone with dental acrylic cement. The exposed bone area was protected with elastomer resin. After surgery, mice received a daily dose of enrofloxacin (10 mg/kg, Centrovet) for five days and supplementary analgesia with ketoprofen (5 mg/kg, Centrovet) for three days. The animals were recovered at least one week before head-fixed training.

4.4.2 In vivo electrophysiological recordings

Before electrophysiological recordings, the mice were habituated at fixation. The mice were fixed twice each day for four days. The fixation time increased daily (15 min, 30min, 1hr, and 1.5 hr.). Every 15 minutes, the mice could drink a solution of sucrose at 30%. At the recording day, craniotomies were made following The Mouse Brain Atlas (Franklin & Paxinos, 2008). For craniotomies surgery, mice were anesthetized with isoflurane (4% induction and 1.5 - 2% maintenance) and placed on a stereotaxic frame. The stereotaxic coordinates used were (relative to Bregma): for the Prefrontal cortex (0.5 mm lateromedial/ +2.0 mm anteroposterior) and CA1 Hippocampus (1.7 mm lateromedial/ -3mm anteroposterior). During the surgery, the temperature was kept at 37° using a heating pad. Two craniotomies were made with a dental drill, accordingly whit the coordinates mentioned above. Once the craniotomies were ready, the electrodes were positioned to record activity in the prefrontal cortex (PFC) and CA1. The cortical regions recorded were Cingulate cortex and Prelimbic Cortex. The hallmark for functional localization of the hippocampus was the firing of CA1 pyramidal cells and the appearance of sharp-waves ripples (SWR). Neuronal activity in the prefrontal cortex was recorded extracellularly with a 32 channel-four shank silicon probe (Neuronexus), stained with

DiI. Neuronal activity in the hippocampus was recorded with a 16 channel-silicon probe stained with DiI and inserted into the brain with a 30° anteroposterior angle. Electrical activity was acquired with a 32-channel Intan RHD 2132 amplifier board connected to an RHD2000 evaluation system (Intan Technologies). FIGURE Nº2 shows the recording sites.

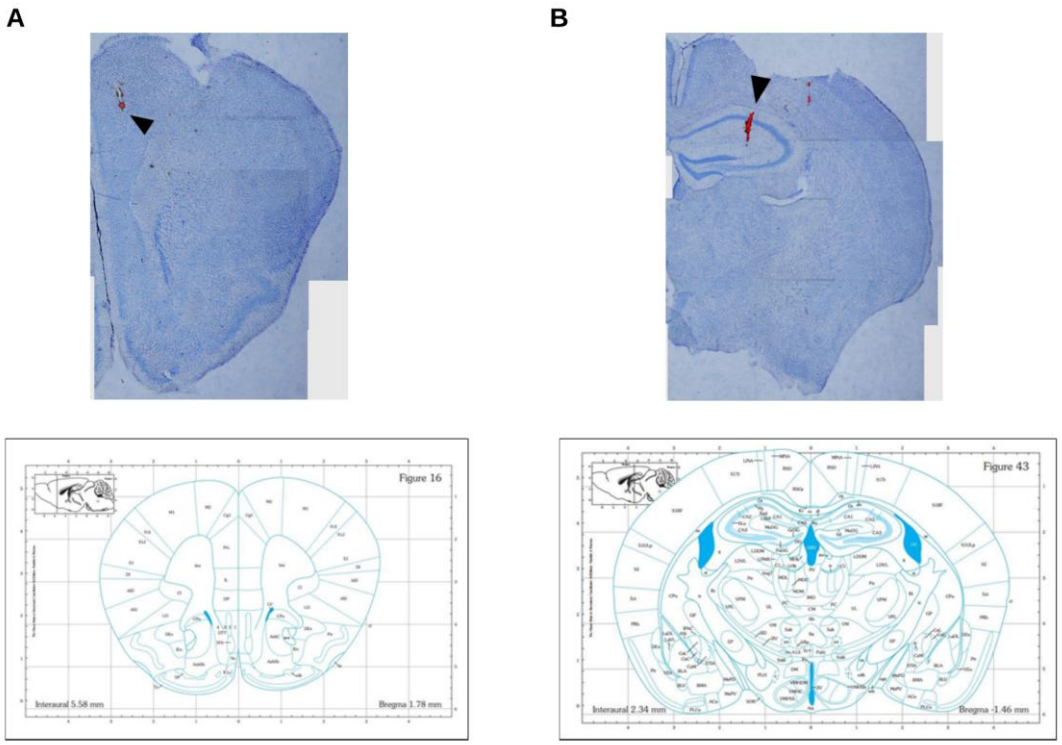

FIGURE Nº2. Representative images from the recording sites. Brain coronal sections from the recorded animals. (A) Recording site from medial Prefrontal Cortex. The top panel shows a photomicrograph of Nissl staining co-localized with DiI staining (red). The black arrowhead shows the DiI staining. (B) Recording site from CA1 layer of the hippocampus. The top panel shows a photomicrograph of Nissl staining co-localized with DiI staining (red). The black arrowhead shows the DiI staining. The bottom panel from both images shows the corresponding area, according to The Mouse Brain Atlas (Franklin & Paxinos, 2008).

4.4.3 Histology

Once finalized the recordings, mice were terminally anesthetized and intracardially perfused with Sodium Chloride 0.9% (NaCl 0.9%) solution followed by Paraformaldehyde 4% (PFA 4%). Brains were extracted and post-fixed in PFA 4% for 24 hours before being transferred to PBS/Sodium Azide 0.2% + Sucrose 30%. Mice brains were sectioned coronally (70 µm slice thickness), and sections were further stained for Nissl staining. The location of the shanks was determined about standard brain atlas coordinates under a light transmission microscope.

4.4.4 Data Analysis

Spike sorting

Spike sorting was performed offline using MATLAB based graphical cluster cutting software, Mclust/Klustakwik-toolbox (version 3.5). In order to detect spikes, broadband recordings sampled at 20 kHz were filtered at 600-5000 Hz. For each recording file, single channels from individual tetrodes were identified, and a single file was generated per channel. All four generated files from the same tetrode were clustered by Principal Components Analysis using MClust 3.5 toolbox running on MATLAB. KlustaKwick automatically identified similar clusters by assigning values between 0.0-1.0 for each cluster, in which similar clusters displayed values close to 1.0. The similarity between clusters was manually confirmed though visual inspection of spike features. Finally, a file for every single unit, including timestamps of spikes for every tetrode, was generated.

Sharp Wave Ripples (SWRs) Detection

The hippocampus local field potential was band-pass filtered (80–200 Hz). Next, the signal was rectified, and low pass filtered at 20 Hz with a 4th order Butterworth filter. This procedure yields a smooth envelope of the filtered signal, which was then z-score normalized using the mean and standard deviation (SD) of the whole signal. The epochs during which the normalized signal exceeded a 3.5 SD threshold were considered as events. Before the threshold, the first point that reached 1 SD was considered the onset, and the first one after the threshold to reach 1 SD as the end of events. The difference between onset and end of events was used to estimate the SWR duration. We introduced a 50-ms-refractory window to prevent double detections. To precisely determine the mean frequency, amplitude, and duration of each event, we performed a spectral analysis using Morlet complex wavelets of 7 cycles. The MATLAB toolbox used is available online as LANtoolbox (http://lantoolbox.wikispaces.com/), which is mostly based on Chronux (www.chronux.org) and FieldTrip (http://fieldtrip.fcdonders.nl/) software toolboxes.

Cross-correlation analysis

The activity of PFC neurons and hippocampal SWR was cross-correlated by applying the “sliding-sweeps” algorithm (Abeles & Gerstein, 1988). A time window of ±1 s was defined with the 0 lag-time assigned to the start time of an SWR. The timestamps of the PFC neuronal spikes within the time window were considered a template and represented by a vector of spikes number relative to t = 0 s, with a time bin of 50 milliseconds and normalized to the total number of spikes. Thus, the

vector's central bin contained the ratio between the number of PFC neuronal spikes elicited between ± 25 milliseconds and the total number of spikes within the template. Next, the window was shifted to successive SWR throughout the recording session, and an array of recurrences of templates was obtained. Both PFC neuronal spikes timestamps and start times of SWR were shuffled by a randomized exchange of the original inter-event intervals (Nádasdy et al., 1999), and the cross-correlation procedure was performed on the pseudo-random sequence. The statistical significance of the observed repetition of spike sequences was assessed by comparing, bin to bin, the original sequence with the shuffled sequence. An original correlation sequence that presented a statistical distribution different from 1000 simulated shuffling was considered statistically significant, with $P < 0.05$ probability, instead of chance occurrence.

Coherence analysis

For analysis of oscillatory activity's power, the electrophysiological recording was down-sampled to 1000 Hz, bandpass-filtered at 0.1–100 Hz, and coherence was computed using multitaper Fourier analysis from the Chronux toolbox (http://www.chronux.org). For spectral coherence, field potentials were divided into 2000 milliseconds segments with 100 milliseconds overlap and a time-bandwidth product of 5 and 9 tapers. Mean spectral power and coherence measures were calculated for theta (4–10 Hz).

4.5 Immunofluorescence staining

Mice were anesthetized with a mix of xylazine, ketamine, and acepromazine (4:4:1, v:v:v), then perfused with a peristaltic bomb (Velp Scientifica SP311) with 100 ml of ice-cold PBS and later with 50 ml of PFA 4%. Brains were removed and post-fixed with PFA 4% at 4ºC overnight, followed by Sucrose 30% in PBS at 4ºC overnight. The brains were cut in 25 µm coronal sections with a cryostat (Leica CM1850).

Immunofluorescence was done on floating sections. We select sections from different areas of the brain, mainly the hippocampus and prefrontal cortex. We wash the sections three times with PBS 1X for 10 minutes per time. After that, we permeabilized sections with Triton X-100 0.4% for 30 minutes. Then, we incubate with Glycine 0.15 M for 15 minutes. Next, we incubated with NaBH4 10 mg/mL prepared at the moment, for 15 minutes. After, we washed with PBS 1X for 10 minutes and incubated with NH4Cl 50mM for 10 minutes. After that, we wash three times with PBS 1X, for 10 minutes per time. Next, the sections were incubated with blocking solution (BS) (Triton X-100 0.4% + BSA 3%) for 1 hour. After BS incubation, we incubated with the primary antibody anti-WO2 (1:1000 dilution) overnight at 4°C. The next day, the primary antibody was withdrawn, and sections were washed three times for 10 minutes per time. After that, the sections were incubated with anti-mouse 488, the AlexaFluor-conjugated secondary antibody (1: 1000 dilution) for two hours at room temperature. Once finished, the sections were washed three times for 15 minutes per time. Finally, the sections were mounted on a slide until they dried, covered with mounting medium and put the coverslip over them.

Fluorescence images were captured under a Nikon Timelapse Microscope at the Unidad de Microscopía Avanzada of the Pontificia Universidad Católica de Chile. The same experiment's images were always acquired using the same settings. Images were quantified using the free access software ImageJ (Fiji) and its plugins. The protocol used for the analysis was developed by the Unidad de Microscopía Avanzada. Briefly, the total image was separated into individual images to facilitate their manipulation, and images were converted to 8bit (monochrome) for segmentation. Images were improved by eliminating the background signal, and then the green signal was segmented on the background to delimit and obtain the total area. The unspecified signal was eliminated, and finally, the number of plaques and the area of each plaque were quantified. This analysis was made by a person blinded to the treatment conditions.

4.6 Statistics

Data sets were tested for normality using the Kolmogorov-Smirnov test and then compared with the appropriate test. All statistical tests were performed using GraphPad Prism 8 software (GraphPad Software, San Diego, CA, USA), except the cross-correlation analysis that was made using MATLAB (The MathWorks, USA). All data are expressed as mean ± SEM.

Behavioral and electrophysiological data were analyzed using one-way ANOVA, two-way ANOVA, Kruskal-Wallis, and one-sample t-test in each corresponding case. The cross-correlation data was analyzed using a bin to bin Kruskal-Wallis test.

Plaques area and plaques number were analyzed using a t-test. All statistical assessments were considered significant when $p<0.05$.

5 RESULTS

5.1 Objective 1. Evaluate the effect of the absence of c-Abl on learning and memory in APP/PS1-Abl-KO mice.

To assess the cognitive status and the effect of the ablation of c-Abl in cognitive performance, we evaluated a battery of behavioral tests that could mainly depend on or not of the hippocampal activity. The Object Location Memory (OLM) task is a hippocampal-dependent test that evaluates spatial memory (Murai et al., 2007). Here we used the factor Recognition Index (RI) to evaluate mice's capacity to recognize the displaced object. We found that WT mice at 10-month-old cannot identify the displaced object (one-sample t-test, $p=0.9102$). Also, as expected, the APP/PS1 aged mice cannot recognize the moving object (one-sample t-test, $p=0.9217$). Interestingly, we found that the aged Abl-KO and the APP/PS1/Abl-KO mice could identify the moving object (one-sample t-test, $p=0.0009$, and $p=0.0006$, respectively). Also, there is a significant difference between APP/PS1/Abl-KO mice and WT and APP/PS1 groups (one-way ANOVA, $p=0.0095$, Tukey's multiple comparison test, $p<0.05$) (FIGURE Nº3). Those data suggest that the absence of c-Abl improves a subset of spatial memory: remember objects and their position in the space. Notice that even in healthy mice, the deficiency of c-Abl improves the performance.

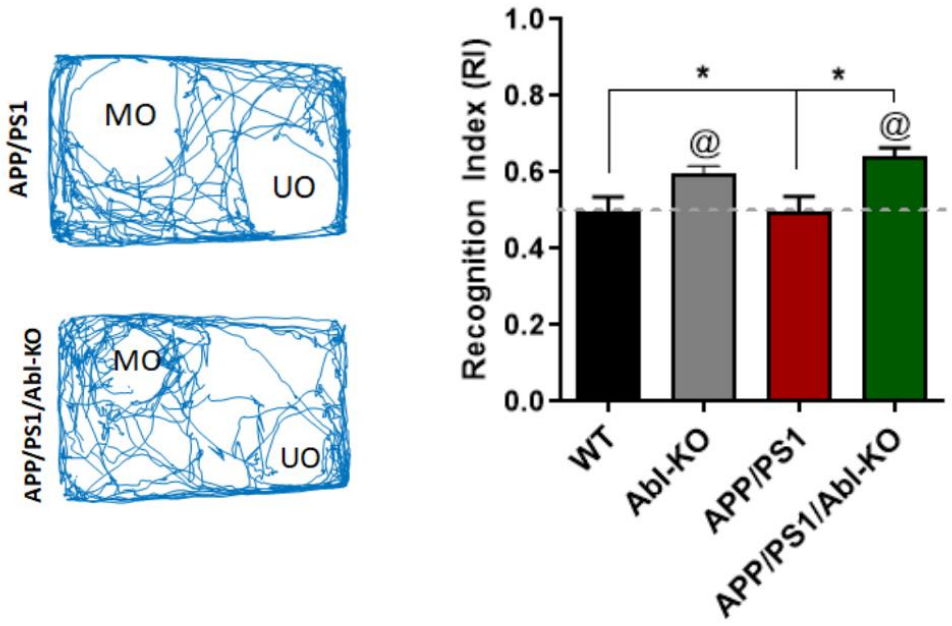

FIGURE Nº3. Object Location Memory test. The bars in the right panel show the time spent in the relocated object, compared to the total time of exploration. The dotted line represents the chance. The left panel shows a representative example of the traveled path. one-way ANOVA, p=0.0095, Tukey's multiple comparison test, *=p<0.05; @ mean significative different from 0.5, the chance. MO: Moved Object. UO: Unmoved Object. WT(n=10), Abl-KO (n=11), APP/PS1 (n=10), APP/PS1/Abl-KO (n=9). The data are presented as mean ± SEM.

We also evaluated a test like the OLM, the Novel Object Recognition (NOR) test. The NOR task is a hippocampus-independent test used to evaluate rodents' recognition memory (Antunes & Biala, 2012). Here we used the factor RI to measure the capacity to recognize the novel object. We found that aged WT mice could recognize the novel object (one-sample t-test, p=0.0055). However, as expected, the APP/PS1 mice did not recognize the novelty of the space (one-sample t-test, p=0.4299). Also, the Abl-KO mice and APP/Abl-KO mice did not recognize the novel object (one-sample t-test, p=0.4436, and p=0.8870, respectively). Finally, we did not find a significant difference between groups (one-way ANOVA, p=0.1366) (FIGURE Nº4). It is interesting to notice that when we compare only WT vs. APP/PS1, we actually can see a difference between groups (FIGURE Nº4, insert), indicating that APP/PS1 mice, the model of AD, has a deficit in the NOR tests, as has been previously reported (Zhang et al., 2012). In contrast with the previous result, a hippocampus-dependent task, the data indicate that the lack of c-Abl does not affect recognition memory.

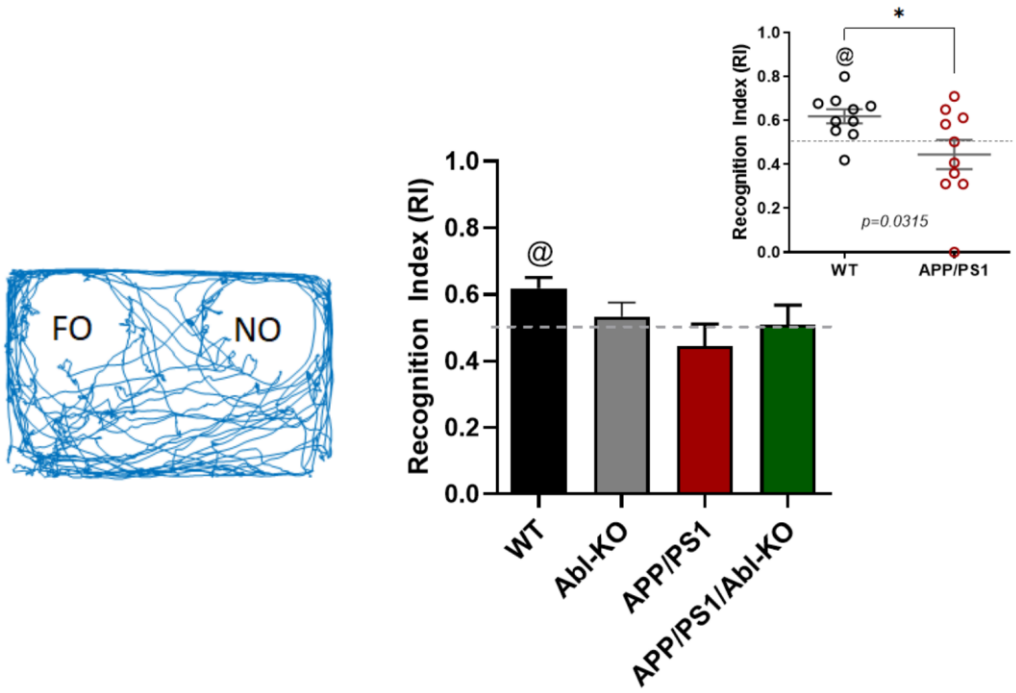

FIGURE Nº4. Novel Object Recognition test. The bars in the right panel show the time spent in the new object, compared to the total time of exploration. The dotted line represents the chance. The left panel shows a representative example of the traveled path. One-way ANOVA, p=0.1366; @ mean significative different from 0.5, the chance. The insert shows a comparison between the WT group and the APP/PS1 group, t-test, p=0,0315. FO: Familiar Object. NO: Novel object. WT(n=10), Abl-KO (n=11), APP/PS1 (n=10), APP/PS1/Abl-KO (n=9). The data are presented as media ± SEM.

Next, we evaluated another hippocampus-dependent task, the Barnes Maze test (BM), that assesses spatial learning and memory in rodents (Sunyer et al., 2007). Here we measure the latency to the target hole (escape hole) through four days. A significant difference between the first day and the other three days it is an indicator of learning. Here we found that aged WT mice had a significantly reduced latency between the day first and day four (two-way ANOVA, days effect: $p<0.0001$, Tukey's multiple comparison test, $p<0.05$). In contrast, as expected, the APP/PS1 mice did significantly differ in the performance between the days (two-way ANOVA, days effect: $p<0.0001$, Tukey's multiple comparison test, $p>0.05$). Interestingly, the aged Abl-KO mice show a marked difference in their performance since day two (two-way ANOVA, days effect: $p<0.0001$, Tukey's multiple comparison test, $p<0.0001$). Further, the APP/PS1/Abl-KO mice had a significantly reduced latency between the day first and day four (two-way ANOVA, days effect: $p<0.0001$, Tukey's multiple comparison test, $p<0.01$). The APP/PS1/Abl-KO group and Abl-KO group have less latency than the WT group in the whole performance regardless of the acquisition day (two-way ANOVA, genotype effect: $p=0.0011$) (FIGURE Nº5). These data indicate, in the first place, that the lack of c-Abl improves spatial learning. Secondly, Abl-KO mice learn faster than WT mice. Finally, APP/PS1/Abl-KO mice's performance is better than APP/PS1 mice, even better than WT mice. Accordingly, as in the OLM task, we can see a similar pattern on how the absence of c-Abl improves memory performance in a hippocampus-dependent task, not only in the context of Alzheimer's disease, in non-pathological one too.

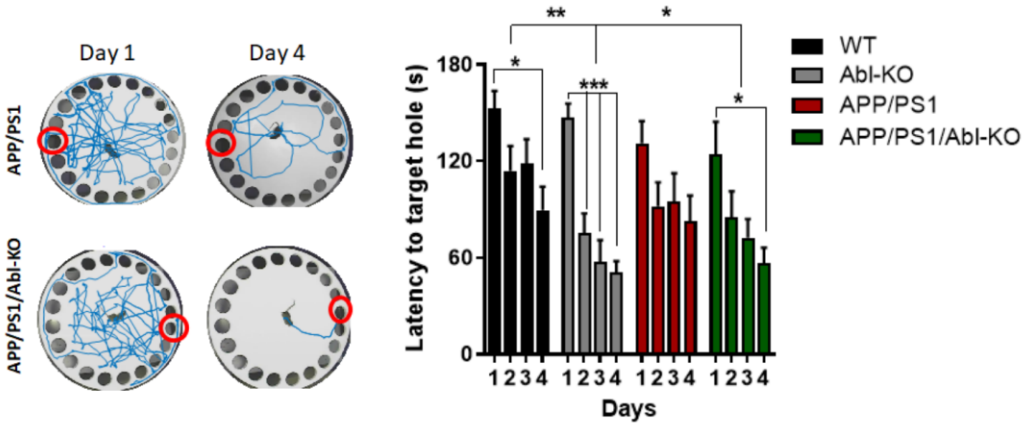

FIGURE Nº5. **Barnes Maze test.** The bars in the right panel show the time spent in finding the target hole each day. The left panel shows a representative example of the traveled path for APP/PS1 and APP/PS1/Abl-KO. two-way ANOVA, days effect: $p<0.0001$, genotype effect: $p=0.0011$. Tukey's multiple comparison test, *=$p<0.05$, **=$p<0.01$, ***=$p<0.001$. WT(n=10), Abl-KO (n=11), APP/PS1 (n=10), APP/PS1/Abl-KO (n=9). The data are presented as mean ± SEM.

To evaluate the general motor activity of mice, we assessed an Open Field test (Seibenhener & Wooten, 2015). The Open Field is an empty arena where the animal can explore for 10 minutes. The most common parameters measured in this test are traveled distance and time spent in a defined zone. The traveled distance is an indicator of locomotor activity, whereas the time spent in the center zone is an indicator of anxiety-like behavior (Seibenhener & Wooten, 2015). Here we did not find any differences between groups either in locomotor activity (one-way ANOVA, $p=0.8534$) or anxiety-like behavior (one-way ANOVA, $p=0.1662$), discarding any motor disability or basal stress (FIGURE Nº6). Thus, the differences showed here are just the product of cognitive processes.

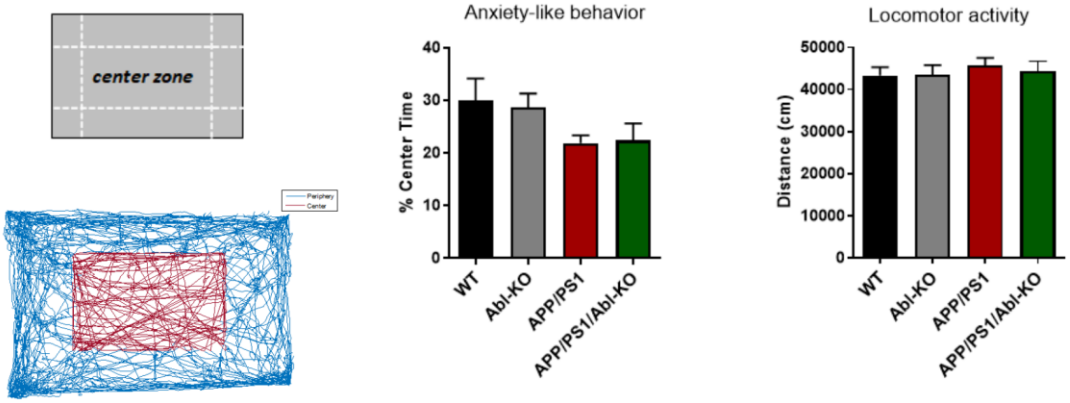

FIGURE Nº6. Open Field test. In each case, the bar shows the percent of time spent exploring the center zone (Anxiety-like behavior) and the distance traveled during the whole exploratory time (basal locomotor activity). The left panel shows a representative example of the traveled path. One-way ANOVA, p=0.1662 (Anxiety-like behavior), p=0.8534 (Locomotor activity). WT(n=10), Abl-KO (n=11), APP/PS1 (n=10), APP/PS1/Abl-KO (n=9). The data are presented as mean ± SEM.

Finally, we decided to add the Memory Flexibility (MF) test, which was not included in the original project, to increase our data's robustness in the hippocampus-dependent tasks. The MF test is a variation of the Morris Water Maze and has seen to be more sensitive to hippocampal dysfunction (Chen et al., 2000). The set of animals used here was different from the set used in the tests mentioned above (see Materials and Methods sections for more details). Also, these animals were older, which allows us to see a better effect associated with Alzheimer's disease since in some water-based spatial working memory tasks, cognitive impairment is present after 10-month-old (Lalonde et al., 2005; Ma et al., 2012; Zhang et al., 2011).

We measured the number of trials to reach the criterion (three consecutive trials with latencies less than 20 seconds) in four consecutive days. Each day of testing, we changed the platform position to the next subsequent quadrant. FIGURE Nº7 left shows the progression in each platform position. We found that the WT mice needed few trials to reach the criterion (5.56 ± 3.18, from 15 trials per day). In contrast, the APP/PS1 mice needed almost all trials (11.46 ± 4.67, from 15 trials per day) to reach the criterion. Similarly to the WT group, the Abl-KO group needs few trials to reach the criterion (5.54 ± 3.16, from 15 trials per day). Interestingly, APP/PS1/Abl-KO mice need almost half of the total trials to reach the criterion (7.38 ± 4.18, from 15 trials per day). Summarizing, we found that the WT group, Abl-KO group, and APP/PS1/Abl-KO group needed fewer trials to reach the criterion than the APP/PS1 group (Kruskal-Wallis test, $p<0.0001$, Tukey's multiple comparison test, $p<0.05$)(FIGURE Nº7, right). As in Barnes Maze and OLM test, the data of the Memory Flexibility suggest that the lack of c-Abl improves hippocampus-dependent

memory. The APP/PS1/Abl-KO mice's performance is better than APP/PS1 mice and does not differ from the WT performance. A difference from the other two tests, here the Abl-KO mice do not differ from the WT mice.

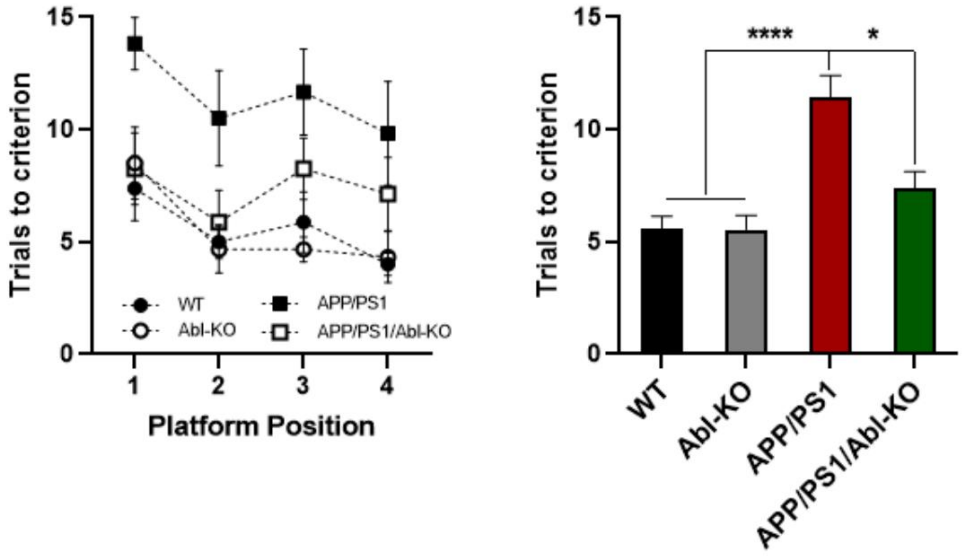

FIGURE Nº7. **Memory Flexibility test.** The bars in the right panel show the number of trials needed to find the hidden platform. The left panel shows the progression in each platform position. The platform position is different each day. Kruskal-Wallis test, $p<0.0001$, Tukey's multiple comparison test, *=$p<0.05$, ****=$p<0.0001$. WT(n=8), Abl-KO (n=6), APP/PS1 (n=6), APP/PS1/Abl-KO (n=8). The data are presented as mean ± SEM.

Taking together all the previous data, we could suggest that the effect of the lack of c-Abl on cognition is selective, having more impact on memories that depends on the hippocampus.

5.2 Objective 2. Evaluate the effect of the absence of c-Abl on functional connectivity between the Prefrontal Cortex and Hippocampus in APP/PS1-Abl-KO mice in resting-state

Because the relationship between the prefrontal cortex and hippocampus is a leading factor in the consolidation and organization of memory networks, we wondered whether the effects of the absence of the c-Abl on learning were related to functional connectivity changes between those areas. To address this objective, we performed simultaneous recordings in the medial prefrontal cortex (mPFC) and the dorsal CA1 hippocampus in awake head-fixed animals from the four groups, after two weeks of performing the behavioral tasks.

We record a total of 12 animals (134 recordings) and were divided as follow: WT, four animals (40 recordings); Abl-KO, three animals (41 recordings); APP/PS1, two animals (18 recordings); and APP/PS1/Abl-KO, three animals (35 recordings).

In the first place, we assess if the lack of c-Abl affects the hippocampus and the prefrontal cortex individually. To achieve these, we evaluated the firing rate of the units recorded as a measure of the neuronal activity in the mPFC. We record 696 units, of which 73.56 % correspond to putative pyramidal cells, and 26.44% correspond to putative interneurons. Figure SUPPLEMENTARY Nº1 shows the waveform characteristics of pyramidal cells and interneurons of all units recorded

regardless of the genotype, and as expected, we get more percentage of putative pyramidal cells than putative interneurons cells. Here we did not find a significant difference when comparing firing rates between groups (Kruskal Wallis test, p=0.187) (FIGURE Nº8, upper panel). Also, when we compare by type of neurons, putative pyramidal or putative interneurons, neither have a difference between groups (FIGURE Nº8, lower panel). These data suggest that the absence of c-Abl did not affect the basal activity in the mPFC. However, we found an unexpected result since the APP/PS1 group did not differ from the WT group.

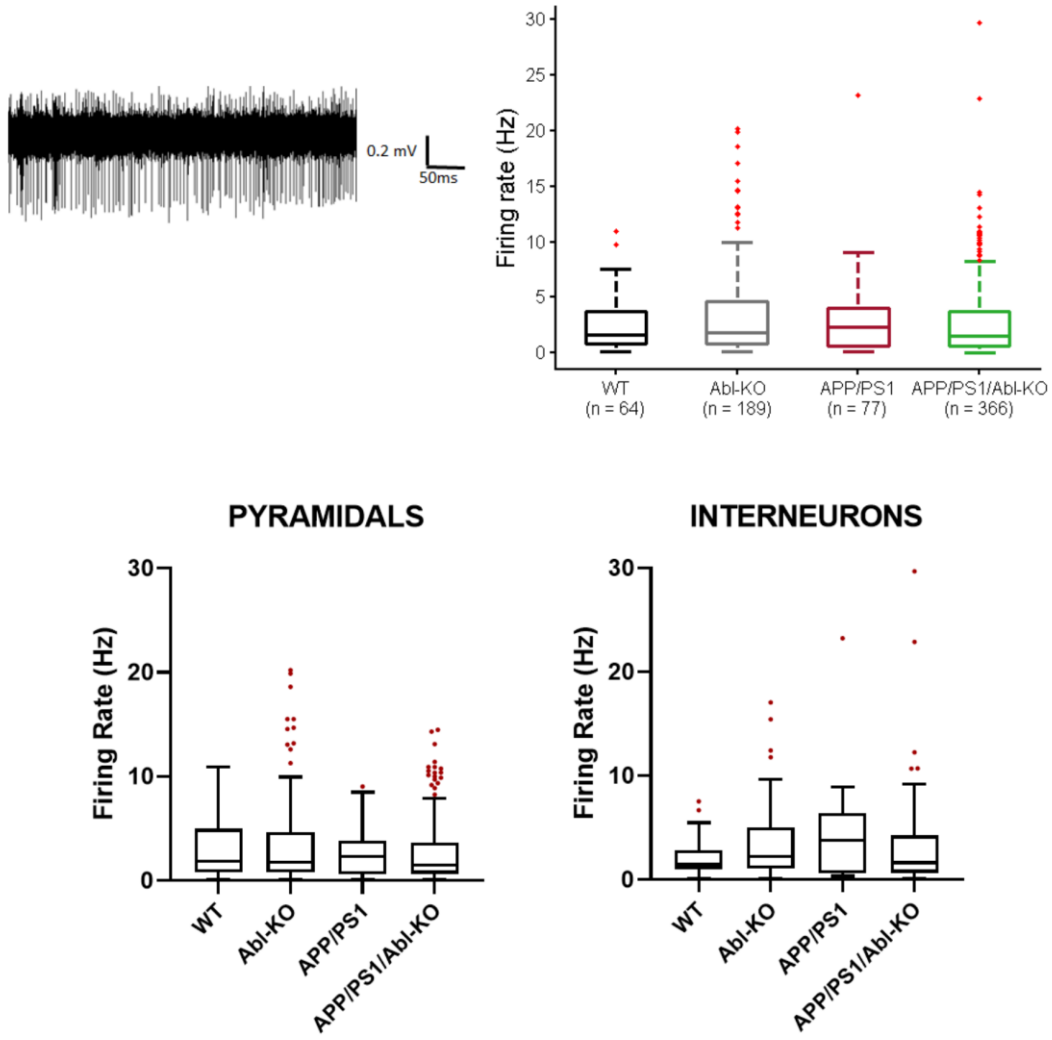

FIGURE Nº8. Neuronal activity in the Prefrontal Cortex. The right upper panel shows the basal firing rate of the neurons. The numbers in parentheses show the unit number per group. The left upper panel shows an example of a multi-unit recording. The lower panel shows a comparison between group by type of neurons, putative pyramidal, and putative interneurons. Kruskal-Wallis, p=0.187 (upper panel), p=0.3995 (pyramidals), p=0.2936 (interneurons). The data are presented as a boxplot. The red dots represent the outliers.

Also, we evaluated the functional integrity of the hippocampus through the sharp-wave ripples (SWRs). The SWRs are oscillations specific to the hippocampus and are related to the transference of memories to the neocortex during memory consolidation (Colgin, 2016). A disruption in any of the ripples features leads to hippocampal impairment, driving cognitive decline (Buzsáki, 2015). Here we evaluated different parameters of the SWRs recorded in the CA1 area of the dorsal hippocampus. The probability of occurrence (or incidence) and frequency are two parameters with an important behavioral correlate. Interrupting the incidence of the SWRs interfere with memory consolidation, whereas the frequency is and indicator of intra-hippocampal connectivity (Buzsáki, 2015).

When we compare the incidence feature between all groups, we obtained a significant difference in the Kruskal-Wallis test ($p=0.0304$). However, Dunn's post-hoc test does not show differences between groups ($p>0.05$) (FIGURE Nº9A). This result could most likely be due to the sample size. However, when we compare independent pairs of groups, we found that WT mice have significative fewer ripples per second than Abl-KO mice (Mann Whitney test, $p=0.0332$). When we performed the comparison between the four groups in the frequency parameter, we found differences only between WT and Abl-KO. The WT mice had significative less frequency than Abl-KO mice (Kruskal-Wallis test, $p=0.0029$, Dunn's multiple comparisons test, $p=0.0059$) (FIGURE Nº9B). Considering those results, we suggest that in physiological conditions, the WT mice present a slightly hippocampal reduced function reflected in a decreased incidence and frequency of ripples. This reduced function is probably related to aging. Interestingly, also in physiological conditions,

the lack of c-Abl increases both parameters, indicating an improvement in the connectivity intra-hippocampus.

Amplitude and duration of the SWRs are also parameters that are often used to describe the hippocampus's functionality. We found a significant difference between animals with (APP/PS1, APP/PS1/Abl-KO), and without (WT, Abl-KO) the AD pathology. AD pathology had deleterious effects on duration (Kruskal-Wallis, $p<0.0001$) and amplitude (Kruskal-Wallis, $p<0.0001$) of the SWRs, in contrast with what we see in the first two parameters (FIGURE Nº9C-D). Contrasting to the incidence and frequency features, we do not see a beneficial effect of the lack of c-Abl in physiological aging. This result suggests that the absence of c-Abl did not impair the amplitude and duration's SWRS features; the impairment is related to the AD pathology.

Taking together, we can suggest a differential effect of the c-Abl on the hippocampus functionality, showing some partial effect only in normal aging.

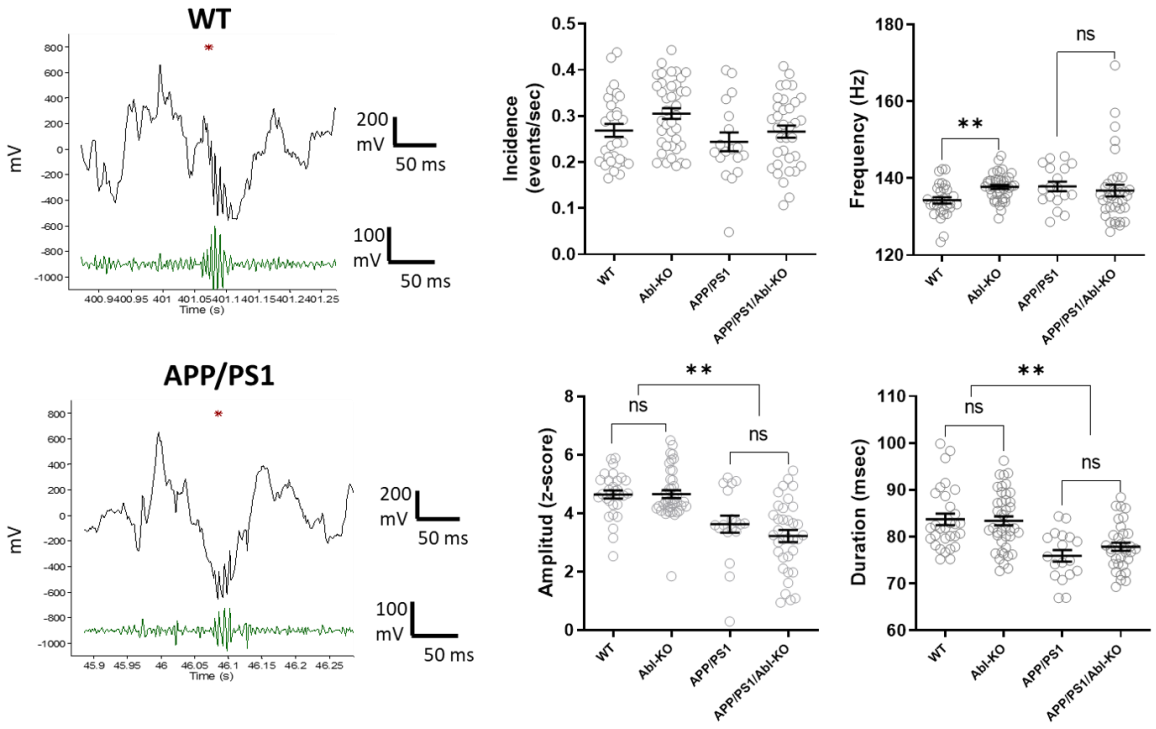

FIGURE Nº9. Sharp-wave ripples parameters. The right panel shows the ripple feature: (A) Incidence, (B) Frequency, (C) Duration, and (D) Amplitude. The left panel show examples of SWR. Red asterisks indicate the onset of the ripple. Kruskal-Wallis test, Dunn's multiple comparison test; ns, no significant; **, p<0.01.

Until now, we showed that our AD model did not present a quantifiable deficit in the prefrontal cortex activity, at least when it is compared with WT littermates. In contrast, we showed a hippocampal dysfunction associated with the disease reflected in a diminished duration and amplitude of the sharp-waves ripples. On the other hand, the absence of c-Abl does not affect PFC's functionality in physiological aging or AD pathology. However, the lack of c-Abl seems to be a favorable effect in the physiological aging's hippocampal activity since it increases incidence and frequency in Abl-KO mice compared with WT mice. Thus, the next steps were to determine if the lack of c-Abl modified the interaction between the hippocampus and prefrontal cortex.

To evaluate the basal functional connectivity in the prefrontal–hippocampal circuit, we use two approaches. First, we compute the normalized cross-correlation function between hippocampal SWRs and neuronal spikes in the mPFC. The cortico-hippocampal coactivation was described previously. A peak near zero in a linear cross-correlation between ripple onset and prefrontal cells is postulated as a mechanism for reorganizing and consolidating neocortical memory traces (Siapas & Wilson, 1998). We observed that neuronal discharge in the mPFC and SWRs in the hippocampus were synchronized (FIGURE Nº10, left). As shown in the cross-correlograms of FIGURE Nº10 (right), we observed a central peak near zero delayed in all the four groups, indicating the simultaneous activation of mPFC neuronal discharge and the hippocampal SWRs (Siapas & Wilson, 1998). The shape of the cross-correlation function was not altered between groups from the onset of SWRs until 200ms. However, from the positive time-lag 200 to 400 ms, mPFC neurons

increased their discharge in APP/PS1 mice. We observed a significant difference between APP/PS1 vs. Abl-KO and APP/PS1 vs. APP/PS1/Abl-KO in a bin to bin comparison (Kruskal- Wallis, *p<0.05) (FIGURE Nº10, right). These differences were not related to the firing rate, given that we found no differences between groups in the mean firing rate of mPFC neurons (FIGURE Nº8). Thus, the increased discharge seems in the APP/PS1 mice could be related to the aberrant excitatory neural activity described previously in AD models (Busche et al., 2008; Palop et al., 2007).

Notice that we also found an increased discharge in the mPFC neurons in WT mice from the time-lag 200 to 400 ms. In wild-type young mice, the cross-correlation function's expected shape is a central peak near zero, followed by a fall (Negrón-Oyarzo et al., 2015). However, it has been shown that aging could lead to pathological hyperexcitability in neurons (H.-L. Wang et al., 2017). Thus, the increased activity seems in our WT mice could be related to an aging feature.

Thus, the data suggest that this alteration in functional connectivity between PFC and hippocampus seems in both physiological aging and AD pathology, improves in the absence of c-Abl.

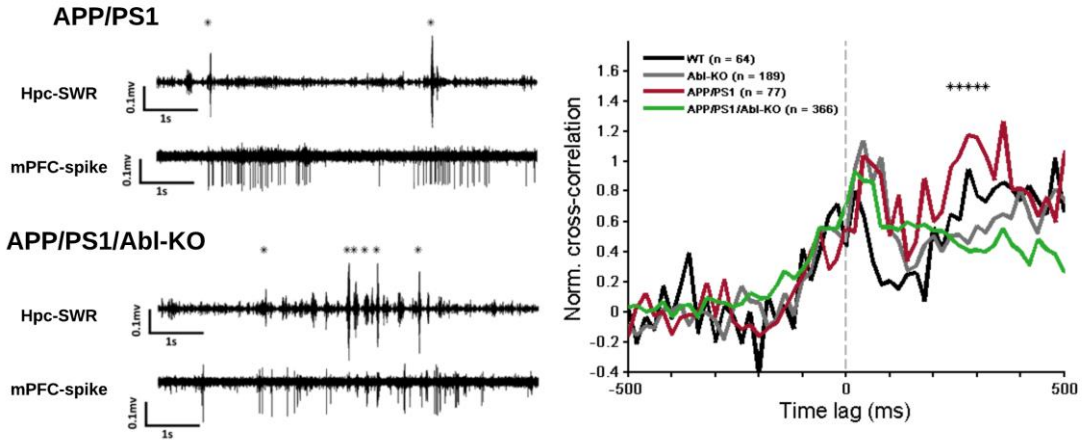

FIGURE Nº10. Cross-correlation analysis. The right panel shows the mean normalized cross-correlation between the significantly correlated mPFC single units to hippocampal SWRs. The left panel shows example recordings, displaying hippocampal SWR (top) and mPFC single unit (lower). Asterisks indicate SWR cross-correlated with mPFC neuronal spikes. Kruskal-Wallis, bin to bin comparison, *=p<0.05.

The second approach to measure the network's state was to calculate all spectra coherence, emphasizing theta oscillation coherence in the prefrontal–hippocampal circuit. Theta oscillations have been implicated in behavioral states and memory performance (Colgin, 2016), and disrupted neural oscillations contribute to AD's cognitive and behavioral alterations. Although we found a decrease in the global coherence in mice with AD pathology (APP/PS1 and APP/PS1/Abl-KO), we identified a diminished interregional coherence in theta oscillations (4-10 Hz) in APP/PS1 mice (FIGURE Nº11, left). We also found that the WT group had significantly increased coherence than the Abl-KO group and the APP/PS1 group (Kruskal-Wallis, $p<0.0001$, Dunn's multiple comparisons test, $p<0.0001$). The APP/PS1/Abl-KO group also had significative greater coherence than the Abl-KO group and APP/PS1 group (Kruskal-Wallis, $p<0.0001$, Dunn's multiple comparisons test, $p=0.0004$). Interestingly, the is no difference between WT mice and APP/PS1/Abl-KO (Kruskal-Wallis, $p<0.0001$, Dunn's multiple comparisons test, $p>0.9999$) (FIGURE Nº11, right). Summarized, the WT and APP/PS1/Abl-KO mice do not present significative differences, and both are distinct from APP/PS1 and Abl-KO mice. These data suggest that the absence of c-Abl in the context of Alzheimer's disease improve the synchronous activity of theta oscillations.

Overall, the cross-correlation analysis and the synchronous activity have a similar pattern. The c-Abl seems to contribute to the dysfunction in the hippocampus-prefrontal cortex axis present in Alzheimer's disease. Therefore, the genetic ablation of c-Abl could recover the impairment.

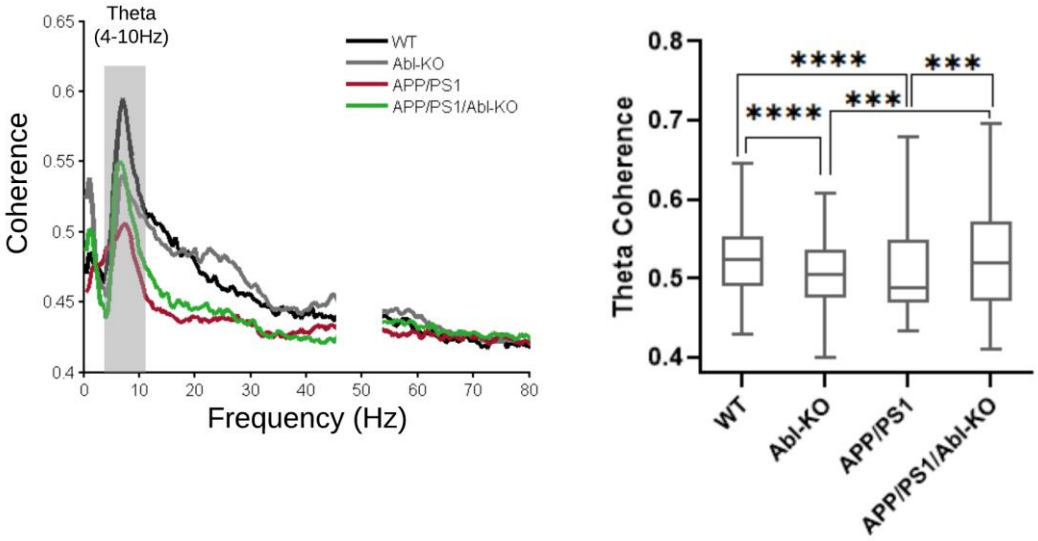

FIGURE Nº11. Coherence analysis. The left panel shows the synchronous activity between the prefrontal cortex and the hippocampus in all the spectra. The gray bar emphasizes the theta oscillation (4-10 Hz). The right panel shows the quantification of the theta coherence. Kruskal-Wallis test, $p<0.0001$, Dunn's multiple comparisons test, ***=$p<0.001$, ****=$p<0.0001$. The data are presented as a boxplot.

5.3 Objective 3. Assess the effect of the absence of c-Abl on β-amyloid plaques in APP/PS1/Abl-KO mice

The β-amyloid aggregations are one of the pathological hallmarks of Alzheimer's disease. The transgenic mouse model used in this project (APPswe/PSEN1Ed9) develops Aβ deposits in the brain by 4-months-old (Garcia-Alloza et al., 2006). We previously have shown that these animals treated with c-Abl inhibitors diminished the brain's Aβ deposits (Cancino et al., 2008). Here, we wanted to evaluate if the genetic ablation of the c-Abl affected Aβ deposition. We measured the amyloid burden in 11-month old mice. As we expected, APP/PS1 mice's brains showed widespread Aβ accumulation and WO2-positive amyloid plaques (FIGURE Nº12A). However, when we compare APP/PS1 vs. APP/PS1/Abl-KO mice, we did not find any differences between groups either in the area or plaques number (t-test, p=0.5588, and p=0.3586, respectively, data not shown). Next, we evaluated the plaque number in younger mice (6-month old) because we previously experienced that APP/PS1 mice treated with Imatinib show decreased plaque burden in younger mice. We found a significant reduction in APP/PS1/Alb-KO mice compared with APP/PS1 mice (t-test, p=0.0119) (FIGURE Nº12B). It is important to notice that the plaque number of younger mice is fewer than the oldest mice. This result is expected since this Alzheimer's disease model develops the senile plaque progressively (Finnie et al., 2017; Garcia-Alloza et al., 2006). Thus, these data suggest that the absence of c-Abl could delay the Aβ aggregation in the AD model.

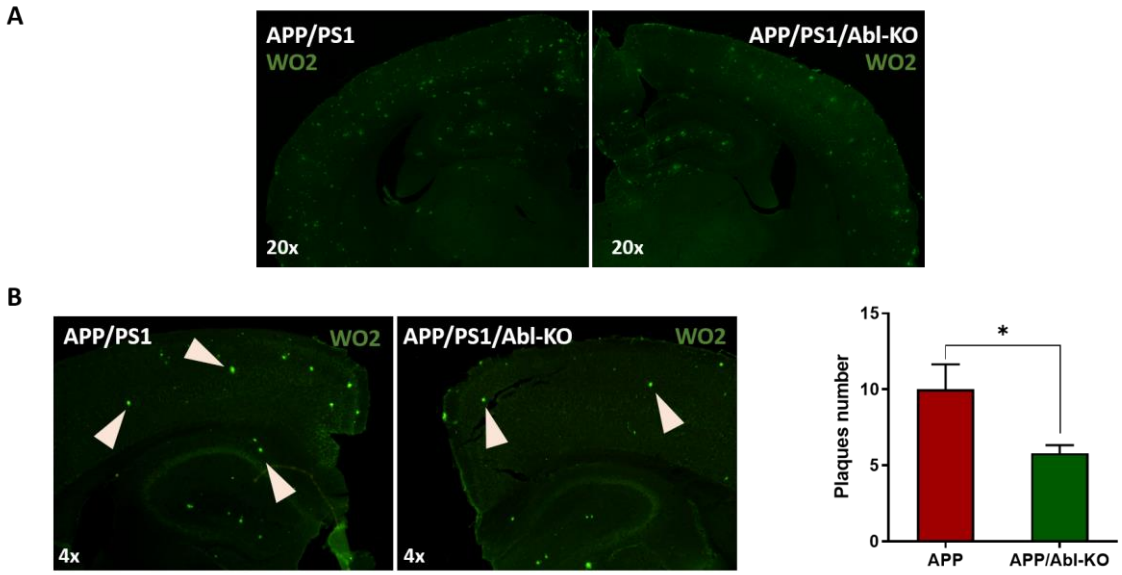

FIGURE Nº12. **Amyloid burden quantification.** (A) 11-month old mice. The panel shows a representative image of the immunofluorescence. Magnification: 20X (B) 6-month old mice. The left panel shows a representative example of the immunofluorescence. White-head arrows show Aβ aggregation. t-test, p=0.0119. We use four animals per group, four slides approximately per animal, ten photos per slide. APP/PS1 (n=4), APP/PS1/Abl-KO (n=4). The data are presented as mean ± SEM.

6 DISCUSSION

6.1 Lack of c-Abl improves behavioral performance in hippocampal-dependent tasks.

In this study, we found that the genetic ablation of c-Abl improves cognitive performance in the hippocampus-dependent task of animals with AD pathology and healthy mice. The hippocampus plays a crucial role in learning, memory, and spatial navigation. This structure is particularly susceptible to damage from epilepsy, hypoxia, ischemia, or encephalitis (Knierim, 2015). In dementia, particularly in Alzheimer's disease, the hippocampus is the first to show senile plaques and tau tangles. Parameters that are well correlated with the cognitive decline in these patients (Lane et al., 2018). Also, hippocampal lesions in experimental animals lead to memory impairment in the Morris Water Maze, which is the dominant test for hippocampal function (Vorhees & Williams, 2006).

Here we show how our model of Alzheimer's disease, the APP/PS1 mice (APPswe/PSEN1Ed9), displays a notorious deficiency in recognition memory (Fig. 4, insert) and in different components of spatial memory (FIGURE Nº3, FIGURE Nº5, and FIGURE Nº7), deficiencies reported widely in the literature in the same AD animal model (Cheng et al., 2019; Li et al., 2019; Sierksma et al., 2014). Nevertheless, the APP/PS1/Abl-KO mice have significantly better performance in all

the spatial memory tests, indicating that a lack of c-Abl attenuates Alzheimer's disease pathology in APP/PS1 mice.

Previous research evaluates the c-Abl knockout in other neurodegenerative diseases, specifically in Parkinson's disease (PD) (Ko et al., 2010; Wu et al., 2016). Despite AD and PD are different pathologies, it has some similarities. Both are neurodegenerative diseases, display pathological protein aggregation, and in the late stages of PD, patients may also have mental and behavioral changes (Kalia & Lang, 2015). c-Abl KO mice were used to test the role of c-Abl in a model of PD (MPTP intoxication). In this model, c-Abl KO mice significantly prevent the loss of TH-positive and Nissl-positive neurons following MPTP exposure. Also, KO of c-Abl significantly protects against the loss of striatal TH-positive fibers (Ko et al., 2010). Later, Wu and colleagues use the same PD model, and they arrive at similar results: MPTP mediates the activation of c-Abl, and that the neuron-specific KO of c-Abl prevents MPTP-induced dopaminergic neuronal death (Wu et al., 2016). Both studies show that the absence of c-Abl may have a neuroprotective effect, mitigating dopaminergic neurons' loss in Parkinson's disease (Abushouk et al., 2018). However, this is the first study that knocked out the c-Abl in AD as far as we know.

Further, studies with inhibitors of c-Abl had shown improvement in the cognitive status in animal models of Alzheimer's disease. Our laboratory had previously shown that in two animal models of Alzheimer's disease (rats injected with Aβ and transgenic mice model), treatment with Imatinib, a c-Abl inhibitor, reduces path length and escape latency in the Morris Water maze (Cancino et al., 2008). Our

laboratory also found that Imatinib prevents LTP impairment induced by Aβ oligomers in hippocampal slices (Vargas et al., 2014).

Although we found that the APP/PS1/Abl-KO group had a better performance than the APP/PS1 group in most of the tests performed, we did not observe the same pattern in the NOR test. This result was not unpredictable since the Novel Object Recognition tests and the Object Location Memory test could seem similar, they are not. Both tests assess different types of memory, and subsequently, there are different brain regions involved. The NOR test evaluates recognition memory and the central brain region involved in the perirhinal cortex (Antunes & Biala, 2012). Microinjections of anisomycin, an inhibitor of protein synthesis, in the perirhinal cortex, impaired the object recognition test. However, the same injection on the hippocampus does not affect recognition memory (Balderas et al., 2008). Otherwise, the OLM is a spatial memory task, and the hippocampus is the critical brain region involved (Murai et al., 2007). Previous reports describe rats with hippocampal lesions impaired place memory and context memory (Mumby et al., 2002). Also, Barnes Maze is a well-known hippocampus-dependent task that evaluates spatial learning and memory (Barnes, 1979), as well as the Memory Flexibility test (Chen et al., 2000). Thus, it is not surprising that our results show that in hippocampus-dependent tasks, APP/PS1/Abl-KO mice had better performance than APP/PS1 mice. Mainly for the combination of two reasons. In the first place, the AD pathology begins in the hippocampus and then spread to other brain areas. Second, the c-Abl does not have a similar expression across the brain, and its expression is most prominent in the

hippocampus and cerebellum (*Experiment Detail :: Allen Brain Atlas: Mouse Brain*, n.d.).

Interestingly, here we show that old WT mice do not recognize the displaced object in the OLM test, but the Abl-KO does. It has been shown that in the OLM test, there is a decline in the location index in wild-type aged mice (Wimmer et al., 2012). The mice used in this project were 10-month old approximately, and when we compare the performance with younger mice (4-month old), we observe a significant impairment in recognizing the displaced object in the older mice (SUPPLEMENTARY Nº2). Aging impairs spatial cognitive function in animals and humans. Additionally, the hippocampal function declines in an age-dependent manner (Murai et al., 2007; Wimmer et al., 2012). Therefore, the fact that the Abl-KO mice, an age-matched group, recognize the displaced object, suggests the lack of c-Abl can revert the impairment associated with healthy aging. This result is coherent with previous data that described that Abl-KO young mice had better cognitive performance than age-matched WT mice (González et al., submitted).

Further, the impairment in WT mice in the OLM test seems to be related to the task characteristics. The OLM relies on an animal's innate preference for novelty without additional external reinforcement (Denninger et al., 2018). Barnes maze and the Memory Flexibility tests use negative external reinforcement to promote spatial learning. In each case, rodents look for an escape from an aversive situation, exposed on a brightly-lit platform or immersed in water, respectively (Denninger et al., 2018). Thus, the cognitive decline observed in the WT group performing the OLM is a typical feature in aged WT mice, abolished in more challenging tasks.

6.2 Lack of c-Abl modifies the functional connectivity during resting-state between the prefrontal cortex and hippocampus.

Current evidence suggests that AD affects various functional and structural connectivity networks in the brain, associated with the topography, clinical phenotype, and severity of the disease (Berron et al., 2020). The hippocampus and prefrontal cortex are necessary for learning and memory, and their interactions are critical for memory-guided behavior (Eichenbaum, 2017). Here, we evaluated the basal functional connectivity in the prefrontal–hippocampal circuit of head-fixed animals, through two approaches: first, a cross-correlation between neuronal spikes from mPFC and hippocampal SWRs; second, the synchronous activity between the prefrontal cortex and hippocampus in theta oscillation.

The hippocampal-cortical connectivity in rodents was described by Siapas & Wilson (1998). They demonstrate the existence of temporal correlations between hippocampal ripples and prefrontal cells. Postulating that this coactivation of hippocampal and neocortical pathways may be essential for memory consolidation, during which memories are transferred from short-term hippocampal to longer-term neocortical stores (Siapas & Wilson, 1998). Here, when we compute the cross-correlation analysis between PFC and hippocampus, we found increased activity of the PFC between 200 and 400 ms in APP/PS1 mice, which was not present in the APP/PS1/Abl-KO group (FIGURE Nº10). This increment in the PFC discharge was no related to the firing rate since there is no difference between groups (FIGURE Nº8). Thus, this increased activity could reflect the abnormal excitability of the prefrontal neurons.

In the last years, there is evidence from studies *in vivo* in both human and animal models of AD, showing that neuronal circuits are hyperactive instead of hypoactive, mainly in the early stages of the disease (Busche & Konnerth, 2015). Busche and collaborators use two-photon Ca^{2+} imaging to evaluate the spontaneous ongoing activity of cortical neurons in a mouse model of Alzheimer's disease. They found out that 21% of neurons displayed an unexpected increase in spontaneous Ca^{2+} transients' frequency. These "hyperactive" neurons were found only near the plaque border, whereas silent cells and cells with regular Ca^{2+} transients were distributed throughout the cortex. They also found that the spontaneous and glutamate-induced Ca^{2+} transients detected in hyperactive neurons were very similar to those recorded in the "normal" neurons, indicating the absence of any significant increase in intrinsic excitability of hyperactive neurons. Finally, they figured out that the hyperactivity appeared to be due to a relative decrease in synaptic inhibition (Busche et al., 2008). They concluded that not only do hyperactive neurons fire more frequently, they also do this in a correlated manner, thus increasing the risk for seizure-like activity. In the same sense, a previous report that evaluated the neuronal activity in an animal model of amyloidosis found a hypersynchronous BOLD signal when evaluating functional connectivity through fMRI. This hypersynchrony was reduced with treatment with antibodies anti-Aβ, suggesting that de Aβ could be related to this process (Shah et al., 2016).

The hyperactive pattern has also been described in hippocampal neurons. Neuronal activity in the plaque-bearing CA1 region of older mice is profoundly altered, with a marked increase in the hyperactive neurons fraction. Interestingly, in the

hippocampus of young mice, a selective increase in hyperactive neurons occurs before forming plaques, suggesting that soluble species of Aβ may underlie this impairment. The acute treatment with a γ-secretase inhibitor that reduces soluble Aβ levels rescued neuronal dysfunction (Busche et al., 2012).

Moreover, BACE activity inhibition reduced prefibrillar Aβ surrounding plaques, rescuing neuronal hyperactivity, impaired long-range circuit function, and memory defects. The functional neuronal impairments reappeared after the infusion of soluble Aβ, mechanistically linking Aβ pathology to neuronal and cognitive dysfunction (Keskin et al., 2017). Related to this, our laboratory has shown that the absence of c-Abl or its inhibition decreases APP's amyloidogenic processing, reducing Aβ levels and oligomerization (Estrada et al., 2016). Being able to establish a link with the fact that the absence of c-Abl diminishes the hypersynchrony observed in Alzheimer's disease’s animal model.

On the other hand, theta oscillations have been implicated in behavioral states and memory performance (Colgin, 2016), and disrupted neural oscillations contribute to AD's cognitive and behavioral alterations. Also, theta oscillation-mediated interactions between the hippocampus and prefrontal cortex are essential for spatial memory (Tamura et al., 2017). Thus, we evaluated the synchronous activity between the prefrontal cortex and hippocampus in all the spectrum but focusing on the theta oscillation. Our data showed a diminished theta coherence in APP/PS1 mice, recovered in APP/PS1/Abl-KO mice (FIGURE Nº11).

Previously, the decreased coherence, amplitude, and power in theta oscillations in animal models of Alzheimer pathology has been reported. Stoiljkovic et al. recorded neural activity in TgF344-AD rats, a transgenic model of Alzheimer's disease. Under urethane anesthesia, TgF344-AD rats showed a significant age-dependent decline in hippocampal theta oscillation. In the freely behaving condition, the power of hippocampal theta oscillation was significantly lower in TgF344-AD rats. These rats showed impaired coherence in both intercortical and hippocampal–cortical network dynamics (Stoiljkovic et al., 2019). Earlier, Tanninen et al. found that despite histologically normal tissues, the dorsal HPC and mPFC of tau-expressing rats showed a significant attenuation of stimulus-evoked theta oscillations (Tanninen et al., 2017). Also, Ahnaou et al. found an early decline of EEG theta oscillations and coherent activity between the PFC and HPC CA1 and severe impairments in theta–gamma oscillations coupling in P301L mice that show tau pathology (Ahnaou et al., 2017).

The data showed here are in basal condition since the animals are in resting-state. It is known that theta oscillations mediate the temporal coordination of hippocampal–prefrontal cortex activity for coherent coding of spatial position during memory-guided behavior (Zielinski et al., 2019). However, some reports evaluate theta oscillations in resting-state (Schutte et al., 2017), REM sleep (Boyce et al., 2016), or under anesthesia (Stoiljkovic et al., 2019). The strength of hippocampal-prefrontal synchrony is correlated with behavioral performance. In this sense, the increased basal coherence in theta oscillation seems in our APP/PS1/Abl-KO mice could be

relevant in the improvement in the memory-guided behavior (see behavioral results above, (FIGURE Nº3, FIGURE Nº5, and FIGURE Nº7).

Deficits in functional connectivity are also described in patients with Alzheimer's disease. Studies of default mode network (DMN) and other resting-states networks have shown a correlation with those networks and dementia severity (Wood, 2014). Accordingly, reduction in functional connectivity is in parallel with a worse Clinical Dementia Rating test. Also, functional connectivity changes have been seen in both sporadic and autosomal AD (Thomas et al., 2014). Recently, it has been described that Aβ accumulation preferentially starts in the core regions of the DMN. The earliest Aβ accumulation is further associated with dysfunctional connectivity within the DMN and between the DMN and the frontoparietal network (Palmqvist et al., 2017).

We also determined the effect of the lack of c-Abl on both the prefrontal cortex and hippocampus, separately. We did not find a difference between groups corresponding to the prefrontal cortex activity (FIGURE Nº8). However, we have an unexpected result because our data do not show that the disease affects prefrontal cortex activity. Our results differ from other authors, where shows how in Aβ-injected rats, there is a decline in PFC activity, resulting in decreased firing rate and diminished functional connectivity in the PFC network (Wei et al., 2015).

Because the sharp-waves ripples are oscillations pattern specific to the hippocampus, we evaluate the hippocampus's functionality through the SWRs. The SWRs play an essential role in memory consolidation processes, and its disruption causes memory deficits in hippocampal-dependent memory task (Girardeau et al.,

2009; Girardeau & Zugaro, 2011). We found that the presence of Alzheimer's pathology affected the amplitude and duration of the SWRs. Still, how Aβ affects the ripples it is not entirely understood. Previous research with animal models of Alzheimer's disease demonstrated that the effect of Aβ on SWRs depends on different factors such as the animal's age and the transgenic model use in the experiment (Hermann et al., 2009; Jura et al., 2019; Nicole et al., 2016). However, it is an agreement that the presence of Aβ leads to synaptic transmission impairment (Kamenetz et al., 2003).

Interesting, Abl-KO mice show an increment in the frequency of the SWRs compare to WT mice (FIGURE Nº9B). It is well established that the ripples' frequency is a marker of the inter-hippocampal connectivity (Buzsáki, 2015). The strengthened connection between the hippocampus translates into improvements in behavioral tasks, particularly those that depend on the hippocampus, which is not only true for aging mice but also for younger ones (González et al., submitted).

The experiments shown here are in resting-state, which means that the animals are awake, but there is no behavioral testing associated with the recordings. Sharp-waves ripples are related to memory consolidation during slow-wave sleep (Joo & Frank, 2018). However, it has been shown that awake SWR also contributes to multiple functions, including learning, retrieval, consolidation, and trajectory planning (Buzsáki, 2015). A critical feature of awake SWRs is the fidelity of recapitulated experience, as accurate portraits of established trajectories are crucial for rapid memory-driven behavioral performance (Roumis & Frank, 2015). Shantanu and colleagues observed a specific learning and performance deficit that

persisted throughout the training associated with awake SWR activity. Consistent with this, there is a link between awake SWRs and hippocampal memory processes, suggesting that awake replay of memory-related information during SWRs supports learning and memory-guided decision-making (Jadhav et al., 2012). The evidence supports the hypothesis that SWR replay during the waking state serves to support retrieval and planning, whereas SWR replay during sleep is prepared to consolidate a memory trace into a gradually broader framework of existing memories.

6.3 Lack of c-Abl slows down the accumulations of Aβ plaques in the brain of APP/PS1/Abl-KO mice.

The extracellular accumulation of the amyloid-β peptide (Aβ), known as senile plaque, is a significant histopathological marker of Alzheimer's disease (Atwood & Bowen, 2015). Here we show that, at 11-month old, we do not see differences between groups. However, at 6-month old, APP/PS1/Abl-KO mice have significantly less amyloid plaque than APP/PS1 mice (FIGURE Nº12). This data suggests that the absence of c-Abl could delay the Aβ aggregation in the model of AD. The same pattern was described by Richard et al. (2008) in a distinct animal model of Alzheimer's disease. They knocked out the toll-like receptor 2 (TLR2), related to the microglial response to AD, and compare the amyloid load at different time points. The findings were that APP-TLR2-KO has less amyloid load than APP mice at 3-month and 6-month old. However, when comparing the groups at 9-month old, the plaque formation difference was attenuated (Richard et al., 2008).

Some studies evaluated the genetic ablation of kinases in animal models of Alzheimer's disease. One report showed that p38 MAPK (p38 mitogen-activated protein kinases) knockout reduced Aβ levels in both the hippocampus and cortex of AD transgenic mice, even as early as 4-months of age (Schnöder et al., 2016). The p38 MAPK is susceptible to stress stimuli, and similarly to c-Abl, its active form has been detected in the brains of AD patients (Schnöder et al., 2016). Another report shows that the IRAK4-KO (Interleukin receptor-associated kinase-4 knockouts) decreased Aβ levels in a murine model of AD (Cameron et al., 2012).

The basis of how c-Abl delay the Aβ accumulations is not entirely understood. However, our laboratory has previously shown that the *in vitro* model of AD treated with Imatinib, a c-Abl inhibitor, displays decreased processing of APP (amyloid-β protein precursor) through the amyloidogenic pathway, which may explain the decrease of Aβ oligomers observed *in vivo* (Estrada et al., 2016). The mechanism underlying this effect could involve APP phosphorylation. In cell cultures expressing the active form of c-Abl, APP is phosphorylated on tyrosine. Thus, Estrada et al. propose that APP phosphorylation could increase APP interaction with BACE (β-site amyloid precursor protein cleaving enzyme), the initiating enzyme in Aβ genesis. Imatinib might prevent the altered trafficking of phosphorylated APP to early endosomes and lysosomes, where BACE is located (Estrada et al., 2016).

6.4 Mechanism Proposal

Our data showed that in an animal model of Alzheimer's disease, the genetic ablation of c-Abl prevents the mice's cognitive performance. The lack of c-Abl diminished the

deficits observed in hippocampus-dependent tasks. Accordingly, when we evaluated the functional connectivity in the hippocampal-prefrontal cortex axis, we also observed that the lack of c-Abl improves AD impairment. Still, how the c-Abl interact to modifies the interplay between the hippocampus and prefrontal cortex?

It is well established that Aβ impairs synaptic plasticity mechanisms, including long-term potentiation (LTP)(Puzzo et al., 2017). The modulation of synaptic glutamate mechanisms mediated by Aβ induced a shift in the excitatory-inhibitory balance (Harris et al., 2020). Impaired glutamate synapses might subsequently lead to increased synaptic activation of NMDA receptors and subsequent desensitization, followed by internalization of NMDARs and AMPA receptors. The receptors' endocytosis leads to LTP's impairment, facilitation of LTD, and spine loss (Harris et al., 2020).

Vargas and colleagues showed that amyloid-β oligomers (AβOs) activate the c-Abl kinase in dendritic spines of hippocampal neurons and that c-Abl kinase activity is required for AβOs-induced synaptic loss. The EphA4 receptor tyrosine kinase is upstream of c-Abl activation by AβOs and EphA4 activation increases in cultured neurons and synaptoneurosomes exposed to AβOs in the brain of Alzheimer-transgenic mice. More interestingly, EphA4/c-Abl activation is a key-signaling event that mediates the synaptic damage induced by AβOs (Vargas et al., 2014). These results are consistent with EphA4 being a novel receptor that mediates synaptic damage induced by AβOs (Matsui et al., 2012).

Recently, Gutierrez and colleagues found that in the presence of AβOs, c-Abl participates in synaptic contact removal, increasing susceptibility to AβOs damage. Its deficiency increases the immature spine population reducing AβOs-induced synapse elimination (Gutierrez et al., 2019).

With the results showed here and the antecedents described above, we suggest the following mechanism proposal (FIGURE Nº13): In the context of Alzheimer's disease, the c-Abl leads synaptic damage such as LTP impairment, dysfunction in the dendritic spine density, as well as a reduction in synaptic clustering. These synaptic alterations are at the base of the impaired connectivity and synchronous activity between the hippocampus and the prefrontal cortex. Connectivity deficiency is translated into cognitive impairment, reflected in a deficiency performance in hippocampus-dependent tasks.

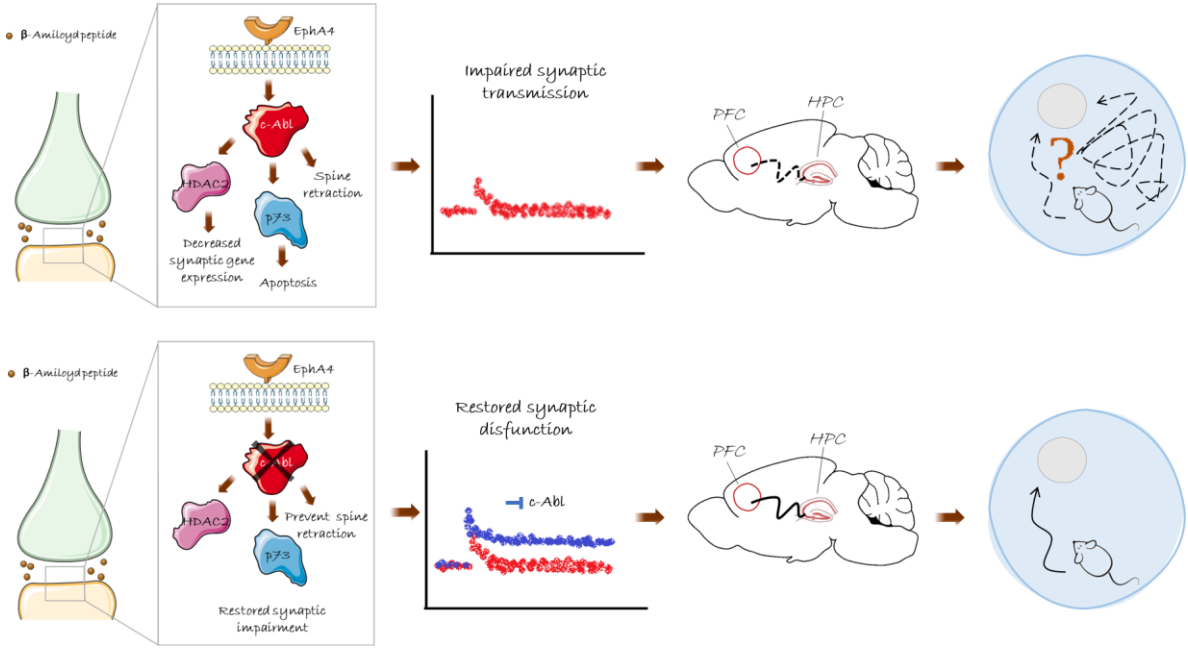

FIGURE Nº13. Mechanism Proposal.

7 CONCLUSIONS

Data presented in this thesis show the relevance of the c-Abl on the progression of Alzheimer's disease. Here we found that whereas APP/PS1 mice show a markedly cognitive deficiency in recognition memory and spatial memory, APP/PS1/Abl-KO mice seem to rescue de damage, mainly in spatial tasks. Interestingly, the Abl-KO mice also rescue the cognitive damage associate with healthy aging.

Additionally, we evaluated the functional connectivity between PFC and hippocampus. When we compute the cross-correlation between both areas, we find and increased discharge in the APP/PS1 mice's PFC. This increased activity was not associated with an increase in the PFC's basal firing rate since there were no differences between groups. This pathological hyperactivity was not found in APP/PS1/Abl-KO mice. We also measure another parameter as an indicator of the state of the network. We found a diminished synchronous activity between PFC and HPC in theta oscillation in APP/PS1 mice. c-APP/PS1Abl ablation recover the impairment associated with the disease.

Finally, we evaluated one of the essential histopathological hallmarks of Alzheimer's disease. We found that the lack of c-Abl in AD mice delay accumulating the amyloid plaques, in comparison with APP/PS1 mice.

In summary, the present work confirms the role of c-Abl on Alzheimer's disease's pathological mechanism, showing, for the first time, data from c-Abl knockout mice in the context of Alzheimer's disease. The data presented proposes the impaired functional connectivity between PFC and HPC as the missing link between the dysfunction at the cellular level and cognitive impairment. These results provide full support to consider the c-Abl as a feasible therapeutic target in Alzheimer's disease.

8 APPENDIX

8.1 TABLE Nº1. Amplification programs for genotypification

	PCR APP/PSEN1	*PCR Abl flox/CRE*
Initial denaturation	94ºC – 10 min.	94ºC – 3 min.
Denaturation	94ºC – 30 sec.	94ºC – 30 sec.
Annealing	57ºC – 1 min.	56ºC – 30 sec.
Extension	72ºC – 1 min.	72ºC – 1 min.
Final Extension	72ºC – 10 min.	72ºC – 1 min.
Hold	4ºC – ∞.	4ºC – ∞.
Cycles	35	38

8.2 TABLE Nº2. Primers sequences

PRIMERS	**SEQUENCES**
APP forward	*5' AGGACTGACCACTCGACCAG 3'*
APP reverse	*5' CGGGGGTCTAGTTCTGCAT 3'*
PSEN1 forward	*5' AATAGAGAACGGCAGGAGCA 3'*
PSEN1 reverse	*5' GCCATGAGGGCACTAATCAT 3'*
c-Abl$^{flox/flox}$ forward	*5' TGTGCATAGCAGGAAGTCCTCCAGAGGA 3'*
c-Abl$^{flox/flox}$ reverse	*5' AGTTAACACACCTCCAGAGTGAGTGCCCT 3'*
CRE forward	*5' GCAAGAACCTGATGGACATGTT 3'*
CRE reverse	*5' GCAATTTCGGCTATACGTAACAGGG 3'*

8.3 Results corresponding to FIGURE Nº8

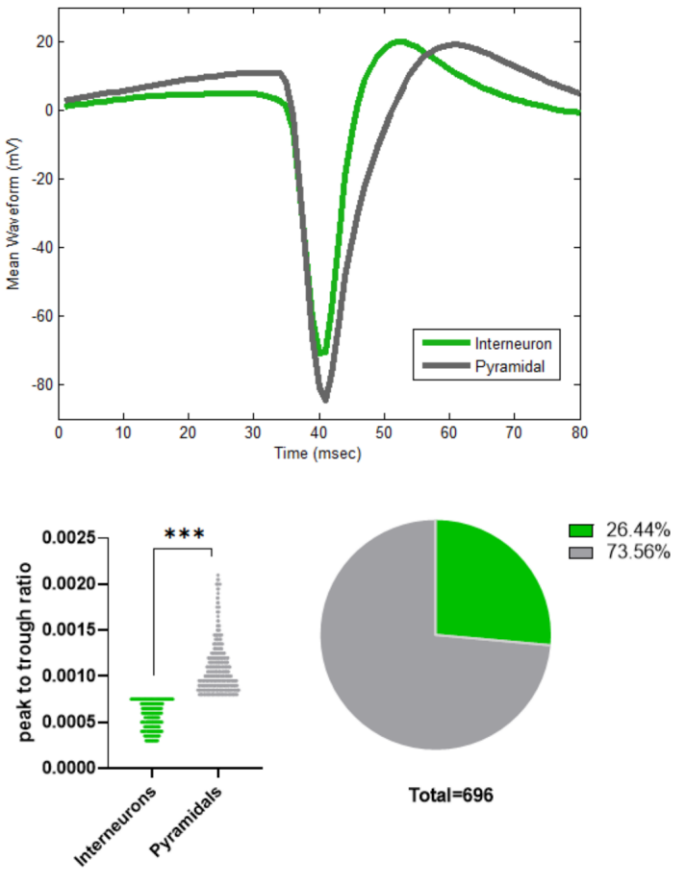

SUPPLEMENTARY Nº1. Waveform characteristics of putative pyramidal cells and putative interneurons recording from medial PCF. The upper panel shows the mean of all waveforms of single units recorded. The lower panel shows the comparison of the peak-to-trough ratio between pyramidal cells and interneurons. As expected, the width of the waveform in interneurons was significantly narrower than in pyramidal cells (Mann-Whitney, $p<0.0001$). The pie chart shows the percentage of units classified as putative pyramidal and interneurons.

8.4 Results corresponding to FIGURE Nº3

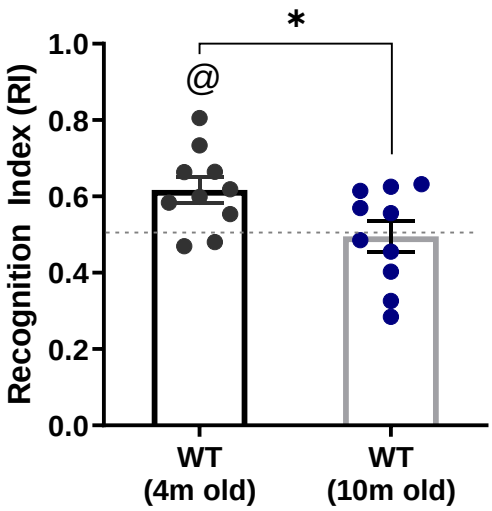

SUPPLEMENTARY Nº2. **Object Location Memory test in young mice.** The bars show the time spent in the relocated object, compared to the total time of exploration. The dotted line represents the chance. t-test, p=0.0303; @ mean significative different from 0.5, the chance. The data are presented as mean ± SEM@, mean different of 0.5.

9 REFERENCES

Abeles, M., & Gerstein, G. L. (1988). Detecting spatiotemporal firing patterns among simultaneously recorded single neurons. *Journal of Neurophysiology*, *60*(3), 909–924. https://doi.org/10.1152/jn.1988.60.3.909

Abushouk, A. I., Negida, A., Elshenawy, R. A., Zein, H., Hammad, A. M., Menshawy, A., & Mohamed, W. M. Y. (2018). C-Abl Inhibition; A Novel Therapeutic Target for Parkinson's Disease. *CNS & Neurological Disorders Drug Targets*, *17*(1), 14–21. https://doi.org/10.2174/1871527316666170602101538

Ahnaou, A., Moechars, D., Raeymaekers, L., Biermans, R., Manyakov, N. V., Bottelbergs, A., Wintmolders, C., Van Kolen, K., Van De Casteele, T., Kemp, J. A., & Drinkenburg, W. H. (2017). Emergence of early alterations in network oscillations and functional connectivity in a tau seeding mouse model of Alzheimer's disease pathology. *Scientific Reports*, *7*(1), 14189. https://doi.org/10.1038/s41598-017-13839-6

Alberici, A., Benussi, A., Premi, E., & Padovani, B. B. and A. (2014). Clinical, Genetic, and Neuroimaging Features of Early Onset Alzheimer Disease: The Challenges of Diagnosis and Treatment. *Current Alzheimer Research*, *11*(10), 909–917. http://www.eurekaselect.com/125933/article

Alvarez, A. R., Klein, A., Castro, J., Cancino, G. I., Amigo, J., Mosqueira, M., Vargas, L. M., Yévenes, L. F., Bronfman, F. C., & Zanlungo, S. (2008). Imatinib

therapy blocks cerebellar apoptosis and improves neurological symptoms in a mouse model of Niemann-Pick type C disease. *FASEB Journal: Official Publication of the Federation of American Societies for Experimental Biology*, *22*(10), 3617–3627. https://doi.org/10.1096/fj.07-102715

Alvarez, A. R., Sandoval, P. C., Leal, N. R., Castro, P. U., & Kosik, K. S. (2004). Activation of the neuronal c-Abl tyrosine kinase by amyloid-β-peptide and reactive oxygen species. *Neurobiology of Disease*, *17*(2), 326–336. https://doi.org/10.1016/j.nbd.2004.06.007

Anderkova, L., Barton, M., & Rektorova, I. (2017). Striato-cortical connections in Parkinson's and Alzheimer's diseases: Relation to cognition. *Movement Disorders*, *32*(6), 917–922. https://doi.org/10.1002/mds.26956

Angel, A., Volkman, R., Royal, T. G., & Offen, D. (2020). Caspase-6 Knockout in the 5xFAD Model of Alzheimer's Disease Reveals Favorable Outcome on Memory and Neurological Hallmarks. *International Journal of Molecular Sciences*, *21*(3), 1144. https://doi.org/10.3390/ijms21031144

Antunes, M., & Biala, G. (2012). The novel object recognition memory: Neurobiology, test procedure, and its modifications. *Cognitive Processing*, *13*(2), 93–110. https://doi.org/10.1007/s10339-011-0430-z

Atwood, C. S., & Bowen, R. L. (2015). A Unified Hypothesis of Early- and Late-Onset Alzheimer's Disease Pathogenesis. *Journal of Alzheimer's Disease: JAD*, *47*(1), 33–47. https://doi.org/10.3233/JAD-143210

Bai, Y., Li, M., Zhou, Y., Ma, L., Qiao, Q., Hu, W., Li, W., Wills, Z. P., & Gan, W.-B. (2017). Abnormal dendritic calcium activity and synaptic depotentiation occur

early in a mouse model of Alzheimer's disease. *Molecular Neurodegeneration*, *12*(1), 86. https://doi.org/10.1186/s13024-017-0228-2

Balderas, I., Rodriguez-Ortiz, C. J., Salgado-Tonda, P., Chavez-Hurtado, J., McGaugh, J. L., & Bermudez-Rattoni, F. (2008). The consolidation of object and context recognition memory involve different regions of the temporal lobe. *Learning & Memory*, *15*(9), 618–624. https://doi.org/10.1101/lm.1028008

Barnes, C. A. (1979). Memory deficits associated with senescence: A neurophysiological and behavioral study in the rat. *Journal of Comparative and Physiological Psychology*, *93*(1), 74–104. https://doi.org/10.1037/h0077579

Bazzigaluppi, P., Beckett, T. L., Koletar, M. M., Lai, A. Y., Joo, I. L., Brown, M. E., Carlen, P. L., McLaurin, J., & Stefanovic, B. (2018). Early-stage attenuation of phase-amplitude coupling in the hippocampus and medial prefrontal cortex in a transgenic rat model of Alzheimer's disease. *Journal of Neurochemistry*, *144*(5), 669–679. https://doi.org/10.1111/jnc.14136

Bero, A. W., Bauer, A. Q., Stewart, F. R., White, B. R., Cirrito, J. R., Raichle, M. E., Culver, J. P., & Holtzman, D. M. (2012). Bidirectional Relationship between Functional Connectivity and Amyloid-β Deposition in Mouse Brain. *Journal of Neuroscience*, *32*(13), 4334–4340. https://doi.org/10.1523/JNEUROSCI.5845-11.2012

Berron, D., van Westen, D., Ossenkoppele, R., Strandberg, O., & Hansson, O. (2020). Medial temporal lobe connectivity and its associations with cognition in early Alzheimer's disease. *Brain*, *143*(4), 1233–1248. https://doi.org/10.1093/brain/awaa068

Bi, D., Wen, L., Wu, Z., & Shen, Y. (2020). GABAergic dysfunction in excitatory and inhibitory (E/I) imbalance drives the pathogenesis of Alzheimer's disease. *Alzheimer's & Dementia: The Journal of the Alzheimer's Association*. https://doi.org/10.1002/alz.12088

Bilkei-Gorzo, A. (2014). Genetic mouse models of brain ageing and Alzheimer's disease. *Pharmacology & Therapeutics*, *142*(2), 244–257. https://doi.org/10.1016/j.pharmthera.2013.12.009

Birnbaum, J. H., Wanner, D., Gietl, A. F., Saake, A., Kündig, T. M., Hock, C., Nitsch, R. M., & Tackenberg, C. (2018). Oxidative stress and altered mitochondrial protein expression in the absence of amyloid-β and tau pathology in iPSC-derived neurons from sporadic Alzheimer's disease patients. *Stem Cell Research*, *27*, 121–130. https://doi.org/10.1016/j.scr.2018.01.019

Boyce, R., Glasgow, S. D., Williams, S., & Adamantidis, A. (2016). Causal evidence for the role of REM sleep theta rhythm in contextual memory consolidation. *Science (New York, N.Y.)*, *352*(6287), 812–816. https://doi.org/10.1126/science.aad5252

Brier, M. R., Thomas, J. B., Snyder, A. Z., Benzinger, T. L., Zhang, D., Raichle, M. E., Holtzman, D. M., Morris, J. C., & Ances, B. M. (2012). Loss of Intranetwork and Internetwork Resting State Functional Connections with Alzheimer's Disease Progression. *Journal of Neuroscience*, *32*(26), 8890–8899. https://doi.org/10.1523/JNEUROSCI.5698-11.2012

Busche, Chen, X., Henning, H. A., Reichwald, J., Staufenbiel, M., Sakmann, B., & Konnerth, A. (2012). Critical role of soluble amyloid-β for early hippocampal hyperactivity in a mouse model of Alzheimer's disease. *Proceedings of the*

National Academy of Sciences of the United States of America, *109*(22), 8740–8745. https://doi.org/10.1073/pnas.1206171109

Busche, Eichhoff, G., Adelsberger, H., Abramowski, D., Wiederhold, K.-H., Haass, C., Staufenbiel, M., Konnerth, A., & Garaschuk, O. (2008). Clusters of Hyperactive Neurons Near Amyloid Plaques in a Mouse Model of Alzheimer's Disease. *Science*, *321*(5896), 1686–1689. https://doi.org/10.1126/science.1162844

Busche, & Konnerth, A. (2015). Neuronal hyperactivity – A key defect in Alzheimer's disease? *BioEssays*, *37*(6), 624–632. https://doi.org/10.1002/bies.201500004

Buzsáki, G. (2015). Hippocampal sharp wave-ripple: A cognitive biomarker for episodic memory and planning. *Hippocampus*, *25*(10), 1073–1188. https://doi.org/10.1002/hipo.22488

Cameron, B., Tse, W., Lamb, R., Li, X., Lamb, B. T., & Landreth, G. E. (2012). Loss of Interleukin Receptor-Associated Kinase 4 Signaling Suppresses Amyloid Pathology and Alters Microglial Phenotype in a Mouse Model of Alzheimer's Disease. *Journal of Neuroscience*, *32*(43), 15112–15123. https://doi.org/10.1523/JNEUROSCI.1729-12.2012

Cancino, G. I., Perez de Arce, K., Castro, P. U., Toledo, E. M., von Bernhardi, R., & Alvarez, A. R. (2011). C-Abl tyrosine kinase modulates tau pathology and Cdk5 phosphorylation in AD transgenic mice. *Neurobiology of Aging*, *32*(7), 1249–1261. https://doi.org/10.1016/j.neurobiolaging.2009.07.007

Cancino, G. I., Toledo, E. M., Leal, N. R., Hernandez, D. E., Yévenes, L. F., Inestrosa, N. C., & Alvarez, A. R. (2008). STI571 prevents apoptosis, tau

phosphorylation and behavioural impairments induced by Alzheimer's β-amyloid deposits. *Brain*, *131*(9), 2425–2442. https://doi.org/10.1093/brain/awn125

Chen, Chen, K. S., Knox, J., Inglis, J., Bernard, A., Martin, S. J., Justice, A., McConlogue, L., Games, D., Freedman, S. B., & Morris, R. G. M. (2000). *A learning deficit related to age and b-amyloid plaques in a mouse model of Alzheimer's disease*. *408*, 5.

Chen, Wang, Z., Tang, B., Fang, M., Li, J., Chen, G., & Wang, X. (2014). Altered expression of c-Abl in patients with epilepsy and in a rat model. *Synapse (New York, N.Y.)*, *68*(7), 306–316. https://doi.org/10.1002/syn.21741

Cheng, W. H., Martens, K. M., Bashir, A., Cheung, H., Stukas, S., Gibbs, E., Namjoshi, D. R., Button, E. B., Wilkinson, A., Barron, C. J., Cashman, N. R., Cripton, P. A., & Wellington, C. L. (2019). CHIMERA repetitive mild traumatic brain injury induces chronic behavioural and neuropathological phenotypes in wild-type and APP/PS1 mice. *Alzheimer's Research & Therapy*, *11*. https://doi.org/10.1186/s13195-018-0461-0

Colgin, L. L. (2016). Rhythms of the hippocampal network. *Nature Reviews Neuroscience*, *17*(4), 239–249. https://doi.org/10.1038/nrn.2016.21

Decker, H., Jürgensen, S., Adrover, M. F., Brito-Moreira, J., Bomfim, T. R., Klein, W. L., Epstein, A. L., Felice, F. G. D., Jerusalinsky, D., & Ferreira, S. T. (2010). N-Methyl-d-aspartate receptors are required for synaptic targeting of Alzheimer's toxic amyloid-β peptide oligomers. *Journal of Neurochemistry*, *115*(6), 1520–1529. https://doi.org/10.1111/j.1471-4159.2010.07058.x

Dementia. (n.d.). Retrieved March 20, 2020, from https://www.who.int/news-room/fact-sheets/detail/dementia

Denninger, J. K., Smith, B. M., & Kirby, E. D. (2018). Novel Object Recognition and Object Location Behavioral Testing in Mice on a Budget. *Journal of Visualized Experiments : JoVE*, *141*. https://doi.org/10.3791/58593

Dorszewska, J., Prendecki, M., Oczkowska, A., Dezor, M., & Kozubski, W. (2016). Molecular Basis of Familial and Sporadic Alzheimer's Disease. *Current Alzheimer Research*, *13*(9), 952–963. https://doi.org/10.2174/1567205013666160314150501

Drummond, E., & Wisniewski, T. (2017). Alzheimer's disease: Experimental models and reality. *Acta Neuropathologica*, *133*(2), 155–175. https://doi.org/10.1007/s00401-016-1662-x

Eichenbaum, H. (2017). Prefrontal–hippocampal interactions in episodic memory. *Nature Reviews Neuroscience*, *18*(9), 547–558. https://doi.org/10.1038/nrn.2017.74

Estrada, & Alvarez, S. M. Z. and A. R. (2011). C-Abl Tyrosine Kinase Signaling: A New Player in AD Tau Pathology. *Current Alzheimer Research*, *8*(6), 643–651. http://www.eurekaselect.com/88615/article

Estrada, L. D., Chamorro, D., Yañez, M. J., Gonzalez, M., Leal, N., von Bernhardi, R., Dulcey, A. E., Marugan, J., Ferrer, M., Soto, C., Zanlungo, S., Inestrosa, N. C., & Alvarez, A. R. (2016). Reduction of Blood Amyloid-β Oligomers in Alzheimer's Disease Transgenic Mice by c-Abl Kinase Inhibition. *Journal of Alzheimer's Disease*, *54*(3), 1193–1205. https://doi.org/10.3233/JAD-151087

Experiment Detail: Allen Brain Atlas: Mouse Brain. (n.d.). Retrieved April 13, 2020, from https://mouse.brain-map.org/experiment/show?id=68844474

Finnie, G. S., Gunnarsson, R., Manavis, J., Blumbergs, P. C., Mander, K. A., Edwards, S., Van den Heuvel, C., & Finnie, J. W. (2017). Characterization of an 'Amyloid Only' Transgenic (B6C3-Tg(APPswe,PSEN1dE9)85Dbo/Mmjax) Mouse Model of Alzheimer's Disease. *Journal of Comparative Pathology*, *156*(4), 389–399. https://doi.org/10.1016/j.jcpa.2017.03.001

Franklin, K. B. J., & Paxinos, G. (2008). *The Mouse Brain in Stereotaxic Coordinates* (Compact 3rd Edition). Elsevier.

Fu, Caprihan, A., Chen, J., Du, Y., Adair, J. C., Sui, J., Rosenberg, G. A., & Calhoun, V. D. (2019). Altered static and dynamic functional network connectivity in Alzheimer's disease and subcortical ischemic vascular disease: Shared and specific brain connectivity abnormalities. *Human Brain Mapping*, *40*(11), 3203–3221. https://doi.org/10.1002/hbm.24591

Fu, Hung, K.-W., Huang, H., Gu, S., Shen, Y., Cheng, E. Y. L., Ip, F. C. F., Huang, X., Fu, W.-Y., & Ip, N. Y. (2014). Blockade of EphA4 signaling ameliorates hippocampal synaptic dysfunctions in mouse models of Alzheimer's disease. *Proceedings of the National Academy of Sciences of the United States of America*, *111*(27), 9959–9964. https://doi.org/10.1073/pnas.1405803111

Garcia-Alloza, M., Robbins, E. M., Zhang-Nunes, S. X., Purcell, S. M., Betensky, R. A., Raju, S., Prada, C., Greenberg, S. M., Bacskai, B. J., & Frosch, M. P. (2006). Characterization of amyloid deposition in the APPswe/PS1dE9 mouse model of Alzheimer disease. *Neurobiology of Disease*, *24*(3), 516–524. https://doi.org/10.1016/j.nbd.2006.08.017

Ghatak, S., Dolatabadi, N., Trudler, D., Zhang, X., Wu, Y., Mohata, M., Ambasudhan, R., Talantova, M., & Lipton, S. A. (2019). Mechanisms of hyperexcitability in Alzheimer's disease hiPSC-derived neurons and cerebral organoids vs isogenic controls. *ELife*, *8*, e50333. https://doi.org/10.7554/eLife.50333

Gimbel, D. A., Nygaard, H. B., Coffey, E. E., Gunther, E. C., Laurén, J., Gimbel, Z. A., & Strittmatter, S. M. (2010). Memory Impairment in Transgenic Alzheimer Mice Requires Cellular Prion Protein. *Journal of Neuroscience*, *30*(18), 6367–6374. https://doi.org/10.1523/JNEUROSCI.0395-10.2010

Girardeau, G., Benchenane, K., Wiener, S. I., Buzsáki, G., & Zugaro, M. B. (2009). Selective suppression of hippocampal ripples impairs spatial memory. *Nature Neuroscience*, *12*(10), 1222–1223. https://doi.org/10.1038/nn.2384

Girardeau, G., & Zugaro, M. (2011). Hippocampal ripples and memory consolidation. *Current Opinion in Neurobiology*, *21*(3), 452–459. https://doi.org/10.1016/j.conb.2011.02.005

Gonzalez-Zuñiga, M., Contreras, P. S., Estrada, L. D., Chamorro, D., Villagra, A., Zanlungo, S., Seto, E., & Alvarez, A. R. (2014). C-Abl Stabilizes HDAC2 Levels by Tyrosine Phosphorylation Repressing Neuronal Gene Expression in Alzheimer's Disease. *Molecular Cell*, *56*(1), 163–173. https://doi.org/10.1016/j.molcel.2014.08.013

Grady, C. L., Furey, M. L., Pietrini, P., Horwitz, B., & Rapoport, S. I. (2001). Altered brain functional connectivity and impaired short-term memory in Alzheimer's disease. *Brain: A Journal of Neurology*, *124*(Pt 4), 739–756. https://doi.org/10.1093/brain/124.4.739

Guntupalli, S., Jang, S. E., Zhu, T., Huganir, R. L., Widagdo, J., & Anggono, V. (2017). GluA1 subunit ubiquitination mediates amyloid-β-induced loss of surface α-amino-3-hydroxy-5-methyl-4-isoxazolepropionic acid (AMPA) receptors. *The Journal of Biological Chemistry*, *292*(20), 8186–8194. https://doi.org/10.1074/jbc.M116.774554

Gutierrez, D. A., Vargas, L. M., Chandia-Cristi, A., de la Fuente, C., Leal, N., & Alvarez, A. R. (2019). C-Abl Deficiency Provides Synaptic Resiliency Against Aβ-Oligomers. *Frontiers in Cellular Neuroscience*, *13*. https://doi.org/10.3389/fncel.2019.00526

Harris, S. S., Wolf, F., De Strooper, B., & Busche, M. A. (2020). Tipping the Scales: Peptide-Dependent Dysregulation of Neural Circuit Dynamics in Alzheimer's Disease. *Neuron*, S0896627320304347. https://doi.org/10.1016/j.neuron.2020.06.005

Hermann, D., Both, M., Ebert, U., Gross, G., Schoemaker, H., Draguhn, A., Wicke, K., & Nimmrich, V. (2009). Synaptic transmission is impaired prior to plaque formation in amyloid precursor protein–overexpressing mice without altering behaviorally-correlated sharp wave–ripple complexes. *Neuroscience*, *162*(4), 1081–1090. https://doi.org/10.1016/j.neuroscience.2009.05.044

Ito, Y., Pandey, P., Mishra, N., Kumar, S., Narula, N., Kharbanda, S., Saxena, S., & Kufe, D. (2001). Targeting of the c-Abl tyrosine kinase to mitochondria in endoplasmic reticulum stress-induced apoptosis. *Molecular and Cellular Biology*, *21*(18), 6233–6242. https://doi.org/10.1128/mcb.21.18.6233-6242.2001

Jackson, R. J., Rudinskiy, N., Herrmann, A. G., Croft, S., Kim, J. M., Petrova, V., Ramos-Rodriguez, J. J., Pitstick, R., Wegmann, S., Garcia-Alloza, M., Carlson, G. A., Hyman, B. T., & Spires-Jones, T. L. (2016). Human tau increases amyloid β plaque size but not amyloid β-mediated synapse loss in a novel mouse model of Alzheimer's disease. *European Journal of Neuroscience*, *44*(12), 3056–3066. https://doi.org/10.1111/ejn.13442

Jadhav, S. P., Kemere, C., German, P. W., & Frank, L. M. (2012). Awake Hippocampal Sharp-Wave Ripples Support Spatial Memory. *Science*, *336*(6087), 1454–1458. https://doi.org/10.1126/science.1217230

Jankowsky, J. L., Fadale, D. J., Anderson, J., Xu, G. M., Gonzales, V., Jenkins, N. A., Copeland, N. G., Lee, M. K., Younkin, L. H., Wagner, S. L., Younkin, S. G., & Borchelt, D. R. (2004). Mutant presenilins specifically elevate the levels of the 42 residue β-amyloid peptide in vivo: Evidence for augmentation of a 42-specific γ secretase. *Human Molecular Genetics*, *13*(2), 159–170. https://doi.org/10.1093/hmg/ddh019

Janus, C., Flores, A. Y., Xu, G., & Borchelt, D. R. (2015). Behavioral abnormalities in APPSwe/PS1dE9 mouse model of AD-like pathology: Comparative analysis across multiple behavioral domains. *Neurobiology of Aging*, *36*(9), 2519–2532. https://doi.org/10.1016/j.neurobiolaging.2015.05.010

Jing, Z., Caltagarone, J., & Bowser, R. (2009). Altered Subcellular Distribution of c-Abl in Alzheimer's Disease. *Journal of Alzheimer's Disease : JAD*, *17*(2), 409–422. https://doi.org/10.3233/JAD-2009-1062

Joo, H. R., & Frank, L. M. (2018). The hippocampal sharp wave–ripple in memory retrieval for immediate use and consolidation. *Nature Reviews Neuroscience*, *19*(12), 744–757. https://doi.org/10.1038/s41583-018-0077-1

Jura, B., Macrez, N., Meyrand, P., & Bem, T. (2019). Deficit in hippocampal ripples does not preclude spatial memory formation in APP/PS1 mice. *Scientific Reports*, *9*(1), 20129. https://doi.org/10.1038/s41598-019-56582-w

Kamenetz, F., Tomita, T., Hsieh, H., Seabrook, G., Borchelt, D., Iwatsubo, T., Sisodia, S., & Malinow, R. (2003). APP Processing and Synaptic Function. *Neuron*, *37*(6), 925–937. https://doi.org/10.1016/S0896-6273(03)00124-7

Karuppagounder, S. S., Brahmachari, S., Lee, Y., Dawson, V. L., Dawson, T. M., & Ko, H. S. (2014). The c-Abl inhibitor, Nilotinib, protects dopaminergic neurons in a preclinical animal model of Parkinson's disease. *Scientific Reports*, *4*(1), 4874. https://doi.org/10.1038/srep04874

Katsumata, R., Ishigaki, S., Katsuno, M., Kawai, K., Sone, J., Huang, Z., Adachi, H., Tanaka, F., Urano, F., & Sobue, G. (2012). C-Abl Inhibition Delays Motor Neuron Degeneration in the G93A Mouse, an Animal Model of Amyotrophic Lateral Sclerosis. *PLOS ONE*, *7*(9), e46185. https://doi.org/10.1371/journal.pone.0046185

Keskin, A. D., Kekuš, M., Adelsberger, H., Neumann, U., Shimshek, D. R., Song, B., Zott, B., Peng, T., Förstl, H., Staufenbiel, M., Nelken, I., Sakmann, B., Konnerth, A., & Busche, M. A. (2017). BACE inhibition-dependent repair of Alzheimer's pathophysiology. *Proceedings of the National Academy of Sciences of the United States of America*, *114*(32), 8631–8636. https://doi.org/10.1073/pnas.1708106114

Khatri, A., Wang, J., & Pendergast, A. M. (2016). Multifunctional Abl kinases in health and disease. *Journal of Cell Science*, *129*(1), 9–16. https://doi.org/10.1242/jcs.175521

Kilgore, M., Miller, C. A., Fass, D. M., Hennig, K. M., Haggarty, S. J., Sweatt, J. D., & Rumbaugh, G. (2010). Inhibitors of Class 1 Histone Deacetylases Reverse Contextual Memory Deficits in a Mouse Model of Alzheimer's Disease. *Neuropsychopharmacology*, *35*(4), 870–880. https://doi.org/10.1038/npp.2009.197

Knierim, J. J. (2015). The hippocampus. *Current Biology*, *25*(23), R1116–R1121. https://doi.org/10.1016/j.cub.2015.10.049

Ko, H. S., Lee, Y., Shin, J.-H., Karuppagounder, S. S., Gadad, B. S., Koleske, A. J., Pletnikova, O., Troncoso, J. C., Dawson, V. L., & Dawson, T. M. (2010). Phosphorylation by the c-Abl protein tyrosine kinase inhibits parkin's ubiquitination and protective function. *Proceedings of the National Academy of Sciences*, *107*(38), 16691–16696. https://doi.org/10.1073/pnas.1006083107

Kodis, E. J., Choi, S., Swanson, E., Ferreira, G., & Bloom, G. S. (2018). N-methyl-D-aspartate receptor-mediated calcium influx connects amyloid-β oligomers to ectopic neuronal cell cycle reentry in Alzheimer's disease. *Alzheimer's & Dementia: The Journal of the Alzheimer's Association*, *14*(10), 1302–1312. https://doi.org/10.1016/j.jalz.2018.05.017

Koelewijn, L., Lancaster, T. M., Linden, D., Dima, D. C., Routley, B. C., Magazzini, L., Barawi, K., Brindley, L., Adams, R., Tansey, K. E., Bompas, A., Tales, A., Bayer, A., & Singh, K. (2019). Oscillatory hyperactivity and hyperconnectivity

in young APOE-ε4 carriers and hypoconnectivity in Alzheimer's disease. *ELife*, *8*, e36011. https://doi.org/10.7554/eLife.36011

Koffie, R. M., Meyer-Luehmann, M., Hashimoto, T., Adams, K. W., Mielke, M. L., Garcia-Alloza, M., Micheva, K. D., Smith, S. J., Kim, M. L., Lee, V. M., Hyman, B. T., & Spires-Jones, T. L. (2009). Oligomeric amyloid β associates with postsynaptic densities and correlates with excitatory synapse loss near senile plaques. *Proceedings of the National Academy of Sciences*, *106*(10), 4012–4017. https://doi.org/10.1073/pnas.0811698106

Koleske, A. J., Gifford, A. M., Scott, M. L., Nee, M., Bronson, R. T., Miczek, K. A., & Baltimore, D. (1998). Essential roles for the Abl and Arg tyrosine kinases in neurulation. *Neuron*, *21*(6), 1259–1272. https://doi.org/10.1016/s0896-6273(00)80646-7

Lalonde, R., Kim, H. D., Maxwell, J. A., & Fukuchi, K. (2005). Exploratory activity and spatial learning in 12-month-old APP695SWE/co+PS1/ΔE9 mice with amyloid plaques. *Neuroscience Letters*, *390*(2), 87–92. https://doi.org/10.1016/j.neulet.2005.08.028

Lane, C. A., Hardy, J., & Schott, J. M. (2018). Alzheimer's disease. *European Journal of Neurology*, *25*(1), 59–70. https://doi.org/10.1111/ene.13439

Larson, M., Sherman, M. A., Amar, F., Nuvolone, M., Schneider, J. A., Bennett, D. A., Aguzzi, A., & Lesné, S. E. (2012). The Complex PrPc-Fyn Couples Human Oligomeric Aβ with Pathological Tau Changes in Alzheimer's Disease. *Journal of Neuroscience*, *32*(47), 16857–16871. https://doi.org/10.1523/JNEUROSCI.1858-12.2012

Laurén, J., Gimbel, D. A., Nygaard, H. B., Gilbert, J. W., & Strittmatter, S. M. (2009). Cellular prion protein mediates impairment of synaptic plasticity by amyloid-β oligomers. *Nature*, *457*(7233), 1128–1132. https://doi.org/10.1038/nature07761

Lee, J. S., Kim, J. H., & Lee, S.-K. (2020). The Relationship between Neuropsychiatric Symptoms and Default-Mode Network Connectivity in Alzheimer's Disease. *Psychiatry Investigation*. https://doi.org/10.30773/pi.2020.0009

Li, C., Shi, J., Wang, B., Li, J., & Jia, H. (2019). CB2 cannabinoid receptor agonist ameliorates novel object recognition but not spatial memory in transgenic APP/PS1 mice. *Neuroscience Letters*, *707*, 134286. https://doi.org/10.1016/j.neulet.2019.134286

Liu, Y., Xu, Y.-F., Zhang, L., Huang, L., Yu, P., Zhu, H., Deng, W., & Qin, C. (2017). Effective expression of Drebrin in hippocampus improves cognitive function and alleviates lesions of Alzheimer's disease in APP (swe)/PS1 (ΔE9) mice. *CNS Neuroscience & Therapeutics*, *23*(7), 590–604. https://doi.org/10.1111/cns.12706

Ma, Du, X., Pick, J. E., Sui, G., Brownlee, M., & Klann, E. (2012). Glucagon-Like Peptide-1 Cleavage Product GLP-1(9-36) Amide Rescues Synaptic Plasticity and Memory Deficits in Alzheimer's Disease Model Mice. *Journal of Neuroscience*, *32*(40), 13701–13708. https://doi.org/10.1523/JNEUROSCI.2107-12.2012

Ma, Gao, Y., Tang, W., Huang, W., & Tang, Y. (2020). Fluoxetine Protects against Dendritic Spine Loss in Middle-aged APPswe/PSEN1dE9 Double Transgenic

Alzheimer's Disease Mice. *Current Alzheimer Research*, *17*(1), 93–103. https://doi.org/10.2174/1567205017666200213095419

Ma, Y., Li, Y., Zong, L.-X., Xing, X.-N., Zhang, W.-G., & Cao, Y.-P. (2011). Improving memory and decreasing cognitive impairment in Tg-APPswe/PSEN1dE9 mice with Aβ3-10 repeat fragment plasmid by reducing Aβ deposition and inflammatory response. *Brain Research*, *1400*, 112–124. https://doi.org/10.1016/j.brainres.2011.05.030

Mahul-Mellier, A.-L., Fauvet, B., Gysbers, A., Dikiy, I., Oueslati, A., Georgeon, S., Lamontanara, A. J., Bisquertt, A., Eliezer, D., Masliah, E., Halliday, G., Hantschel, O., & Lashuel, H. A. (2014). c-Abl phosphorylates α-synuclein and regulates its degradation: Implication for α-synuclein clearance and contribution to the pathogenesis of Parkinson's disease. *Human Molecular Genetics*, *23*(11), 2858–2879. https://doi.org/10.1093/hmg/ddt674

Mañucat-Tan, N. B., Shen, L.-L., Bobrovskaya, L., Al-hawwas, M., Zhou, F. H., Wang, Y.-J., & Zhou, X.-F. (2019). Knockout of p75 neurotrophin receptor attenuates the hyperphosphorylation of Tau in pR5 mouse model. *Aging*, *11*(17). https://doi.org/10.18632/aging.102202

Matsui, C., Inoue, E., Kakita, A., Arita, K., Deguchi-Tawarada, M., Togawa, A., Yamada, A., Takai, Y., & Takahashi, H. (2012). Involvement of the γ-secretase-mediated EphA4 signaling pathway in synaptic pathogenesis of Alzheimer's disease. *Brain Pathology (Zurich, Switzerland)*, *22*(6), 776–787. https://doi.org/10.1111/j.1750-3639.2012.00587.x

Meng, Y., Ding, L., Zhang, H., Yin, W., Yan, Y., & Cao, Y. (2017a). Immunization of Tg-APPswe/PSEN1dE9 mice with Aβ3-10-KLH vaccine prevents synaptic

deficits of Alzheimer's disease. *Behavioural Brain Research*, *332*, 64–70. https://doi.org/10.1016/j.bbr.2017.05.056

Meng, Y., Ding, L., Zhang, H.-Y., Yin, W.-C., Yan, Y., & Cao, Y.-P. (2017b). An Aβ3-10-KLH vaccine reduced Alzheimer's disease-like pathology and had a sustained effect in Tg-APPswe/PSEN1dE9 mice. *Brain Research*, *1673*, 72–77. https://doi.org/10.1016/j.brainres.2017.07.017

Moresco, E. M. Y., Scheetz, A. J., Bornmann, W. G., Koleske, A. J., & Fitzsimonds, R. M. (2003). Abl Family Nonreceptor Tyrosine Kinases Modulate Short-Term Synaptic Plasticity. *Journal of Neurophysiology*, *89*(3), 1678–1687. https://doi.org/10.1152/jn.00892.2002

Mucke, L., & Selkoe, D. J. (2012). Neurotoxicity of Amyloid β-Protein: Synaptic and Network Dysfunction. *Cold Spring Harbor Perspectives in Medicine*, *2*(7), a006338. https://doi.org/10.1101/cshperspect.a006338

Mumby, D. G., Gaskin, S., Glenn, M. J., Schramek, T. E., & Lehmann, H. (2002). Hippocampal Damage and Exploratory Preferences in Rats: Memory for Objects, Places, and Contexts. *Learning & Memory*, *9*(2), 49–57. https://doi.org/10.1101/lm.41302

Murai, T., Okuda, S., Tanaka, T., & Ohta, H. (2007). Characteristics of object location memory in mice: Behavioral and pharmacological studies. *Physiology & Behavior*, *90*(1), 116–124. https://doi.org/10.1016/j.physbeh.2006.09.013

Nádasdy, Z., Hirase, H., Czurkó, A., Csicsvari, J., & Buzsáki, G. (1999). Replay and Time Compression of Recurring Spike Sequences in the Hippocampus. *The Journal of Neuroscience*, *19*(21), 9497–9507. https://doi.org/10.1523/JNEUROSCI.19-21-09497.1999

Negrón-Oyarzo, I., Neira, D., Espinosa, N., Fuentealba, P., & Aboitiz, F. (2015). Prenatal Stress Produces Persistence of Remote Memory and Disrupts Functional Connectivity in the Hippocampal–Prefrontal Cortex Axis. *Cerebral Cortex*, *25*(9), 3132–3143. https://doi.org/10.1093/cercor/bhu108

Nicole, O., Hadzibegovic, S., Gajda, J., Bontempi, B., Bem, T., & Meyrand, P. (2016). Soluble amyloid beta oligomers block the learning-induced increase in hippocampal sharp wave-ripple rate and impair spatial memory formation. *Scientific Reports*, *6*(1), 1–12. https://doi.org/10.1038/srep22728

Oddo, S., Caccamo, A., Shepherd, J. D., Murphy, M. P., Golde, T. E., Kayed, R., Metherate, R., Mattson, M. P., Akbari, Y., & LaFerla, F. M. (2003). Triple-Transgenic Model of Alzheimer's Disease with Plaques and Tangles: Intracellular Aβ and Synaptic Dysfunction. *Neuron*, *39*(3), 409–421. https://doi.org/10.1016/S0896-6273(03)00434-3

Palakurti, R., & Vadrevu, R. (2017). Identification of abelson tyrosine kinase inhibitors as potential therapeutics for Alzheimer's disease using multiple e-pharmacophore modeling and molecular dynamics. *Journal of Biomolecular Structure & Dynamics*, *35*(4), 883–896. https://doi.org/10.1080/07391102.2016.1166454

Palmqvist, S., Schöll, M., Strandberg, O., Mattsson, N., Stomrud, E., Zetterberg, H., Blennow, K., Landau, S., Jagust, W., & Hansson, O. (2017). Earliest accumulation of β-amyloid occurs within the default-mode network and concurrently affects brain connectivity. *Nature Communications*, *8*. https://doi.org/10.1038/s41467-017-01150-x

Palop, J. J., Chin, J., Roberson, E. D., Wang, J., Thwin, M. T., Bien-Ly, N., Yoo, J., Ho, K. O., Yu, G.-Q., Kreitzer, A., Finkbeiner, S., Noebels, J. L., & Mucke, L. (2007). Aberrant Excitatory Neuronal Activity and Compensatory Remodeling of Inhibitory Hippocampal Circuits in Mouse Models of Alzheimer's Disease. *Neuron*, *55*(5), 697–711. https://doi.org/10.1016/j.neuron.2007.07.025

Park, G., Nhan, H. S., Tyan, S.-H., Kawakatsu, Y., Zhang, C., Navarro, M., & Koo, E. H. (2020). Caspase Activation and Caspase-Mediated Cleavage of APP Is Associated with Amyloid β-Protein-Induced Synapse Loss in Alzheimer's Disease. *Cell Reports*, *31*(13), 107839. https://doi.org/10.1016/j.celrep.2020.107839

Peleg, S., Sananbenesi, F., Zovoilis, A., Burkhardt, S., Bahari-Javan, S., Agis-Balboa, R. C., Cota, P., Wittnam, J. L., Gogol-Doering, A., Opitz, L., Salinas-Riester, G., Dettenhofer, M., Kang, H., Farinelli, L., Chen, W., & Fischer, A. (2010). Altered Histone Acetylation Is Associated with Age-Dependent Memory Impairment in Mice. *Science*, *328*(5979), 753–756. https://doi.org/10.1126/science.1186088

Pérez-Escudero, A., Vicente-Page, J., Hinz, R. C., Arganda, S., & de Polavieja, G. G. (2014). idTracker: Tracking individuals in a group by automatic identification of unmarked animals. *Nature Methods*, *11*(7), 743–748. https://doi.org/10.1038/nmeth.2994

Pusil, S., López, M. E., Cuesta, P., Bruña, R., Pereda, E., & Maestú, F. (2019). Hypersynchronization in mild cognitive impairment: The 'X' model. *Brain*, *142*(12), 3936–3950. https://doi.org/10.1093/brain/awz320

Puzzo, D., Piacentini, R., Fá, M., Gulisano, W., Li Puma, D. D., Staniszewski, A., Zhang, H., Tropea, M. R., Cocco, S., Palmeri, A., Fraser, P., D'Adamio, L., Grassi, C., & Arancio, O. (2017). LTP and memory impairment caused by extracellular Aβ and Tau oligomers is APP-dependent. *ELife*, *6*. https://doi.org/10.7554/eLife.26991

Reiserer, R. S., Harrison, F. E., Syverud, D. C., & McDonald, M. P. (2007). Impaired spatial learning in the APPSwe + PSEN1ΔE9 bigenic mouse model of Alzheimer's disease. *Genes, Brain and Behavior*, *6*(1), 54–65. https://doi.org/10.1111/j.1601-183X.2006.00221.x

Reitz, C., Brayne, C., & Mayeux, R. (2011). Epidemiology of Alzheimer disease. *Nature Reviews Neurology*, *7*(3), 137–152. https://doi.org/10.1038/nrneurol.2011.2

Rezaeiasl, Z., Salami, M., & Sepehri, G. (2019). The Effects of Probiotic Lactobacillus and Bifidobacterium Strains on Memory and Learning Behavior, Long-Term Potentiation (LTP), and Some Biochemical Parameters in β-Amyloid-Induced Rat's Model of Alzheimer's Disease. *Preventive Nutrition and Food Science*, *24*(3), 265–273. https://doi.org/10.3746/pnf.2019.24.3.265

Richard, K. L., Filali, M., Prefontaine, P., & Rivest, S. (2008). Toll-Like Receptor 2 Acts as a Natural Innate Immune Receptor to Clear Amyloid 1-42 and Delay the Cognitive Decline in a Mouse Model of Alzheimer's Disease. *Journal of Neuroscience*, *28*(22), 5784–5793. https://doi.org/10.1523/JNEUROSCI.1146-08.2008

Rojas, F., Gonzalez, D., Cortes, N., Ampuero, E., Hernández, D. E., Fritz, E., Abarzua, S., Martinez, A., Elorza, A. A., Alvarez, A., Court, F., & van Zundert, B. (2015). Reactive oxygen species trigger motoneuron death in non-cell-autonomous models of ALS through activation of c-Abl signaling. *Frontiers in Cellular Neuroscience*, *9*. https://doi.org/10.3389/fncel.2015.00203

Rosenberger, A. F., Rozemuller, A. J., van der Flier, W. M., Scheltens, P., van der Vies, S. M., & Hoozemans, J. J. (2014). Altered distribution of the EphA4 kinase in hippocampal brain tissue of patients with Alzheimer's disease correlates with pathology. *Acta Neuropathologica Communications*, *2*, 79. https://doi.org/10.1186/s40478-014-0079-9

Roumis, D. K., & Frank, L. M. (2015). Hippocampal sharp-wave ripples in waking and sleeping states. *Current Opinion in Neurobiology*, *35*, 6–12. https://doi.org/10.1016/j.conb.2015.05.001

Saito, K., Elce, J. S., Hamos, J. E., & Nixon, R. A. (1993). Widespread activation of calcium-activated neutral proteinase (calpain) in the brain in Alzheimer disease: A potential molecular basis for neuronal degeneration. *Proceedings of the National Academy of Sciences*, *90*(7), 2628–2632. https://doi.org/10.1073/pnas.90.7.2628

Schlatterer, S. D., Acker, C. M., & Davies, P. (2011). C-Abl in Neurodegenerative Disease. *Journal of Molecular Neuroscience*, *45*(3), 445–452. https://doi.org/10.1007/s12031-011-9588-1

Schnöder, L., Hao, W., Qin, Y., Liu, S., Tomic, I., Liu, X., Fassbender, K., & Liu, Y. (2016). Deficiency of Neuronal p38α MAPK Attenuates Amyloid Pathology in Alzheimer Disease Mouse and Cell Models through Facilitating Lysosomal

Degradation of BACE1. *Journal of Biological Chemistry*, *291*(5), 2067–2079. https://doi.org/10.1074/jbc.M115.695916

Schumacher, J., Peraza, L. R., Firbank, M., Thomas, A. J., Kaiser, M., Gallagher, P., O'Brien, J. T., Blamire, A. M., & Taylor, J.-P. (2019). Dynamic functional connectivity changes in dementia with Lewy bodies and Alzheimer's disease. *NeuroImage : Clinical*, *22*. https://doi.org/10.1016/j.nicl.2019.101812

Schutte, I., Kenemans, J. L., & Schutter, D. J. L. G. (2017). Resting-state theta/beta EEG ratio is associated with reward- and punishment-related reversal learning. *Cognitive, Affective & Behavioral Neuroscience*, *17*(4), 754–763. https://doi.org/10.3758/s13415-017-0510-3

Scott, L., Feng, J., Kiss, T., Needle, E., Atchison, K., Kawabe, T. T., Milici, A. J., Hajós-Korcsok, É., Riddell, D., & Hajós, M. (2012). Age-dependent disruption in hippocampal theta oscillation in amyloid-β overproducing transgenic mice. *Neurobiology of Aging*, *33*(7), 1481.e13-1481.e23. https://doi.org/10.1016/j.neurobiolaging.2011.12.010

Seibenhener, M. L., & Wooten, M. C. (2015). Use of the Open Field Maze to Measure Locomotor and Anxiety-like Behavior in Mice. *Journal of Visualized Experiments : JoVE*, *96*. https://doi.org/10.3791/52434

Shah, D., Jonckers, E., Praet, J., Vanhoutte, G., Palacios, R. D. y, Bigot, C., D'Souza, D. V., Verhoye, M., & Linden, A. V. der. (2013). Resting State fMRI Reveals Diminished Functional Connectivity in a Mouse Model of Amyloidosis. *PLOS ONE*, *8*(12), e84241. https://doi.org/10.1371/journal.pone.0084241

Shah, D., Praet, J., Latif Hernandez, A., Höfling, C., Anckaerts, C., Bard, F., Morawski, M., Detrez, J. R., Prinsen, E., Villa, A., De Vos, W. H., Maggi, A., D'Hooge, R., Balschun, D., Rossner, S., Verhoye, M., & Van der Linden, A. (2016). Early pathologic amyloid induces hypersynchrony of BOLD resting-state networks in transgenic mice and provides an early therapeutic window before amyloid plaque deposition. *Alzheimer's & Dementia: The Journal of the Alzheimer's Association*, *12*(9), 964–976. https://doi.org/10.1016/j.jalz.2016.03.010

Siapas, A. G., & Wilson, M. A. (1998). Coordinated Interactions between Hippocampal Ripples and Cortical Spindles during Slow-Wave Sleep. *Neuron*, *21*(5), 1123–1128. https://doi.org/10.1016/S0896-6273(00)80629-7

Sierksma, A. S. R., van den Hove, D. L. A., Pfau, F., Philippens, M., Bruno, O., Fedele, E., Ricciarelli, R., Steinbusch, H. W. M., Vanmierlo, T., & Prickaerts, J. (2014). Improvement of spatial memory function in APPswe/PS1dE9 mice after chronic inhibition of phosphodiesterase type 4D. *Neuropharmacology*, *77*, 120–130. https://doi.org/10.1016/j.neuropharm.2013.09.015

Simón, A. M., de Maturana, R. L., Ricobaraza, A., Escribano, L., Schiapparelli, L., Cuadrado-Tejedor, M., Pérez-Mediavilla, A., Avila, J., Del Río, J., & Frechilla, D. (2009). Early changes in hippocampal Eph receptors precede the onset of memory decline in mouse models of Alzheimer's disease. *Journal of Alzheimer's Disease: JAD*, *17*(4), 773–786. https://doi.org/10.3233/JAD-2009-1096

Stoiljkovic, M., Kelley, C., Stutz, B., Horvath, T. L., & Hajós, M. (2019). Altered Cortical and Hippocampal Excitability in TgF344-AD Rats Modeling

Alzheimer's Disease Pathology. *Cerebral Cortex*, *29*(6), 2716–2727. https://doi.org/10.1093/cercor/bhy140

Sunyer, B., Patil, S., Frischer, C., Höger, H., Selcher, J., Brannath, W., & Lubec, G. (2007). Strain-dependent effects of SGS742 in the mouse. *Behavioural Brain Research*, *181*(1), 64–75. https://doi.org/10.1016/j.bbr.2007.03.025

Tamura, M., Spellman, T. J., Rosen, A. M., Gogos, J. A., & Gordon, J. A. (2017). Hippocampal-prefrontal theta-gamma coupling during performance of a spatial working memory task. *Nature Communications*, *8*. https://doi.org/10.1038/s41467-017-02108-9

Tanninen, S. E., Nouriziabari, B., Morrissey, M. D., Bakir, R., Dayton, R. D., Klein, R. L., & Takehara-Nishiuchi, K. (2017). Entorhinal tau pathology disrupts hippocampal-prefrontal oscillatory coupling during associative learning. *Neurobiology of Aging*, *58*, 151–162. https://doi.org/10.1016/j.neurobiolaging.2017.06.024

Thomas, J. B., Brier, M. R., Bateman, R. J., Snyder, A. Z., Benzinger, T. L., Xiong, C., Raichle, M., Holtzman, D. M., Sperling, R. A., Mayeux, R., Ghetti, B., Ringman, J. M., Salloway, S., McDade, E., Rossor, M. N., Ourselin, S., Schofield, P. R., Masters, C. L., Martins, R. N., … Ances, B. M. (2014). Functional Connectivity in Autosomal Dominant and Late-Onset Alzheimer Disease. *JAMA Neurology*, *71*(9), 1111–1122. https://doi.org/10.1001/jamaneurol.2014.1654

Toledo, E. M., & Inestrosa, N. C. (2010). Activation of Wnt signaling by lithium and rosiglitazone reduced spatial memory impairment and neurodegeneration in

brains of an APPswe/PSEN1ΔE9 mouse model of Alzheimer's disease. *Molecular Psychiatry*, *15*(3), 272–285. https://doi.org/10.1038/mp.2009.72

Um, J. W., Nygaard, H. B., Heiss, J. K., Kostylev, M. A., Stagi, M., Vortmeyer, A., Wisniewski, T., Gunther, E. C., & Strittmatter, S. M. (2012). Alzheimer amyloid-β oligomer bound to postsynaptic prion protein activates Fyn to impair neurons. *Nature Neuroscience*, *15*(9), 1227–1235. https://doi.org/10.1038/nn.3178

Vargas, Cerpa, W., Muñoz, F. J., Zanlungo, S., & Alvarez, A. R. (2018). Amyloid-β oligomers synaptotoxicity: The emerging role of EphA4/c-Abl signaling in Alzheimer's disease. *Biochimica et Biophysica Acta (BBA) - Molecular Basis of Disease*, *1864*(4, Part A), 1148–1159. https://doi.org/10.1016/j.bbadis.2018.01.023

Vargas, Leal, N., Estrada, L. D., González, A., Serrano, F., Araya, K., Gysling, K., Inestrosa, N. C., Pasquale, E. B., & Alvarez, A. R. (2014). EphA4 Activation of c-Abl Mediates Synaptic Loss and LTP Blockade Caused by Amyloid-β Oligomers. *PLOS ONE*, *9*(3), e92309. https://doi.org/10.1371/journal.pone.0092309

Volianskis, A., Køstner, R., Mølgaard, M., Hass, S., & Jensen, M. S. (2010). Episodic memory deficits are not related to altered glutamatergic synaptic transmission and plasticity in the CA1 hippocampus of the APPswe/PS1ΔE9-deleted transgenic mice model of β-amyloidosis. *Neurobiology of Aging*, *31*(7), 1173–1187. https://doi.org/10.1016/j.neurobiolaging.2008.08.005

Vorhees, C. V., & Williams, M. T. (2006). Morris water maze: Procedures for assessing spatial and related forms of learning and memory. *Nature Protocols*, *1*(2), 848–858. https://doi.org/10.1038/nprot.2006.116

Vossel, K. A., Ranasinghe, K. G., Beagle, A. J., Mizuiri, D., Honma, S. M., Dowling, A. F., Darwish, S. M., Van Berlo, V., Barnes, D. E., Mantle, M., Karydas, A. M., Coppola, G., Roberson, E. D., Miller, B. L., Garcia, P. A., Kirsch, H. E., Mucke, L., & Nagarajan, S. S. (2016). Incidence and Impact of Subclinical Epileptiform Activity in Alzheimer's Disease. *Annals of Neurology*, *80*(6), 858–870. https://doi.org/10.1002/ana.24794

Wang. (2014). The Capable ABL: What Is Its Biological Function? *Molecular and Cellular Biology*, *34*(7), 1188–1197. https://doi.org/10.1128/MCB.01454-13

Wang, H.-L., Xian, X.-H., Song, Q.-Y., Pang, C., Wang, J.-L., Wang, M.-W., & Li, W.-B. (2017). Age-related alterations of neuronal excitability and voltage-dependent Ca2+ current in a spontaneous mouse model of Alzheimer's disease. *Behavioural Brain Research*, *321*, 209–213. https://doi.org/10.1016/j.bbr.2017.01.009

Wang, Zang, Y., He, Y., Liang, M., Zhang, X., Tian, L., Wu, T., Jiang, T., & Li, K. (2006). Changes in hippocampal connectivity in the early stages of Alzheimer's disease: Evidence from resting state fMRI. *NeuroImage*, *31*(2), 496–504. https://doi.org/10.1016/j.neuroimage.2005.12.033

Wei, J., Yi, H., Zhang, D., & Tian, W. B. and X. (2015). Aberrant Neuronal Activity and Dysfunctional Connectivity in $A\beta_{1–42}$- mediated Memory Deficits in Rats. *Current Alzheimer Research*, *12*(10), 964–973. http://www.eurekaselect.com/136123/article

Wetzler, M., Talpaz, M., Van Etten, R. A., Hirsh-Ginsberg, C., Beran, M., & Kurzrock, R. (1993). Subcellular localization of Bcr, Abl, and Bcr-Abl proteins in normal and leukemic cells and correlation of expression with myeloid differentiation. *The Journal of Clinical Investigation*, *92*(4), 1925–1939. https://doi.org/10.1172/JCI116786

Wills, Z., Marr, L., Zinn, K., Goodman, C. S., & Van Vactor, D. (1999). Profilin and the Abl tyrosine kinase are required for motor axon outgrowth in the Drosophila embryo. *Neuron*, *22*(2), 291–299. https://doi.org/10.1016/s0896-6273(00)81090-9

Wimmer, M. E., Hernandez, P. J., Blackwell, J., & Abel, T. (2012). Aging impairs hippocampus-dependent long-term memory for object location in mice. *Neurobiology of Aging*, *33*(9), 2220–2224. https://doi.org/10.1016/j.neurobiolaging.2011.07.007

Wood, H. (2014). Functional connectivity changes show similar trajectories in autosomal dominant and sporadic Alzheimer disease. *Nature Reviews Neurology*, *10*(9), 483–483. https://doi.org/10.1038/nrneurol.2014.149

Woodring, P. J., Litwack, E. D., O'Leary, D. D. M., Lucero, G. R., Wang, J. Y. J., & Hunter, T. (2002). Modulation of the F-actin cytoskeleton by c-Abl tyrosine kinase in cell spreading and neurite extension. *The Journal of Cell Biology*, *156*(5), 879–892. https://doi.org/10.1083/jcb.200110014

Wu, R., Chen, H., Ma, J., He, Q., Huang, Q., Liu, Q., Li, M., & Yuan, Z. (2016). C-Abl–p38 α signaling plays an important role in MPTP-induced neuronal death. *Cell Death & Differentiation*, *23*(3), 542–552. https://doi.org/10.1038/cdd.2015.135

Xiao, M.-F., Xu, D., Craig, M. T., Pelkey, K. A., Chien, C.-C., Shi, Y., Zhang, J., Resnick, S., Pletnikova, O., Salmon, D., Brewer, J., Edland, S., Wegiel, J., Tycko, B., Savonenko, A., Reeves, R. H., Troncoso, J. C., McBain, C. J., Galasko, D., & Worley, P. F. (2017). NPTX2 and cognitive dysfunction in Alzheimer's Disease. *ELife*, *6*, e23798. https://doi.org/10.7554/eLife.23798

Xu, Y., Yan, J., Zhou, P., Li, J., Gao, H., Xia, Y., & Wang, Q. (2012). Neurotransmitter receptors and cognitive dysfunction in Alzheimer's disease and Parkinson's disease. *Progress in Neurobiology*, *97*(1), 1–13. https://doi.org/10.1016/j.pneurobio.2012.02.002

Zhang, Hao, J., Liu, R., Zhang, Z., Lei, G., Su, C., Miao, J., & Li, Z. (2011). Soluble Aβ levels correlate with cognitive deficits in the 12-month-old APPswe/PS1dE9 mouse model of Alzheimer's disease. *Behavioural Brain Research*, *222*(2), 342–350. https://doi.org/10.1016/j.bbr.2011.03.072

Zhang, Q., Yang, C., Liu, T., Liu, L., Li, F., Cai, Y., Lv, K., Li, X., Gao, J., Sun, D., Xu, H., Yang, Q., & Fan, X. (2018). Citalopram restores short-term memory deficit and non-cognitive behaviors in APP/PS1 mice while halting the advance of Alzheimer's disease-like pathology. *Neuropharmacology*, *131*, 475–486. https://doi.org/10.1016/j.neuropharm.2017.12.021

Zhang, Wang, D., Gong, P., Lin, A., Zhang, Y., Ye, R. D., & Yu, Y. (2019). Formyl Peptide Receptor 2 Deficiency Improves Cognition and Attenuates Tau Hyperphosphorylation and Astrogliosis in a Mouse Model of Alzheimer's Disease. *Journal of Alzheimer's Disease: JAD*, *67*(1), 169–179. https://doi.org/10.3233/JAD-180823

Zhang, Xue, G., Wang, S., Zhang, L., Shi, C., & Xie, X. (2012). Novel Object Recognition as a Facile Behavior Test for Evaluating Drug Effects in AβPP/PS1 Alzheimer's Disease Mouse Model. *Journal of Alzheimer's Disease*, *31*(4), 801–812. https://doi.org/10.3233/JAD-2012-120151

Zhong, Z., Yang, L., Wu, X., Huang, W., Yan, J., Liu, S., Sun, X., Liu, K., Lin, H., Kuang, S., & Tang, X. (2014). Evidences for B6C3-Tg (APPswe/PSEN1dE9) double-transgenic mice between 3 and 10 months as an age-related Alzheimer's disease model. *Journal of Molecular Neuroscience: MN*, *53*(3), 370–376. https://doi.org/10.1007/s12031-013-0203-5

Zhou, Z.-H., Wu, Y.-F., Wang, X., & Han, Y.-Z. (2017). The c-Abl inhibitor in Parkinson disease. *Neurological Sciences*, *38*(4), 547–552. https://doi.org/10.1007/s10072-016-2808-2

Zielinski, M. C., Shin, J. D., & Jadhav, S. P. (2019). Coherent Coding of Spatial Position Mediated by Theta Oscillations in the Hippocampus and Prefrontal Cortex. *The Journal of Neuroscience: The Official Journal of the Society for Neuroscience*, *39*(23), 4550–4565. https://doi.org/10.1523/JNEUROSCI.0106-19.2019

Zott, B., Simon, M. M., Hong, W., Unger, F., Chen-Engerer, H.-J., Frosch, M. P., Sakmann, B., Walsh, D. M., & Konnerth, A. (2019). A vicious cycle of β amyloid-dependent neuronal hyperactivation. *Science (New York, N.Y.)*, *365*(6453), 559–565. https://doi.org/10.1126/science.aay0198